



Lukas Gottsbacher, BSc.

Calculation of the Young's Modulus for Rock Masses with 3DEC and comparing it with empirical methods

Master's Thesis

Submitted in fulfilment of the requirements for the degree of

Diplom-Ingenieur / Diplom-Ingenieurin

Master's programme Civil Engineering, Geotechnics and Hydraulics

at

Graz University of Technology

Supervisor

O.Univ.-Prof. Dipl.-Ing. Dr.mont. Wulf Schubert

Supervising Assistant

Andreas Anjan Buyer, MSc., BSc.

Institute of Rock Mechanics and Tunnelling

Graz University of Technology

Graz, September 2017

EIDESSTATTLICHE ERKLÄRUNG

AFFIDAVIT

Ich erkläre an Eides statt, dass ich die vorliegende Arbeit selbstständig verfasst, andere als die angegebenen Quellen/Hilfsmittel nicht benutzt, und die den benutzten Quellen wörtlich und inhaltlich entnommenen Stellen als solche kenntlich gemacht habe. Das in TUGRAZonline hochgeladene Textdokument ist mit der vorliegenden Masterarbeit identisch.

I declare that I have authored this thesis independently, that I have not used other than the declared sources/resources, and that I have explicitly marked all material which has been quoted either literally or by content from the used sources. The text document uploaded to TUGRAZonline is identical to the present master 's thesis.

Datum / Date

Unterschrift / Signature

Principle of equality

Due to reasons of legibility, this work does not include gender-specific formulations. However, the used male expressions stand for both genders.

Acknowledgements

At this point I would like to thank all those who supported me in the completion of this master thesis as well as in my studies.

I would like to thank my supervisors O.Univ.-Prof. Dipl.-Ing. Dr.mont. Wulf Schubert and Andreas Anjan Buyer, M.Sc., B.Sc. for their very good supervision, as well as Alexander Kluckner M.Sc., B.Sc. for his support with 3DEC.

A special thanks go to the members of the "Wasserbauzeichensaal". I experienced a lot with them and they made this study an amazing experience to me. In particular, I want to thank my fellow students Niko Daurer, Max Fiebich, Claudia Hösele, Johannes Karner and Stefan Leitner, with whom I share a lot of great memories.

Most of all I want to thank my family, especially my parents, without their support I would have never been able to successfully complete my study.

Danksagung

An dieser Stelle möchte ich mich bei all denen bedanken, die mich bei der Fertigstellung dieser Arbeit sowie in meinem Studium unterstützt haben.

Ich möchte mich bei meinen Betreuern O.Univ.-Prof. Dipl.-Ing. Dr.mont. Wulf Schubert und Andreas Anjan Buyer, M.Sc., B.Sc. für die sehr gute Betreuung, sowie bei Alexander Kluckner M.Sc., B.Sc. für seine Unterstützung bei 3DEC bedanken.

Ein spezieller Dank gilt auch den Mitgliedern des Wasserbauzeichensaals, mit denen ich sehr viel erlebt habe und die dieses Studium zu etwas sehr besonderen für mich gemacht haben. Im besonderen möchte ich meinen Kommilitonen Niko Daurer, Max Fiebich, Claudia Hösele, Johannes Karner und Stefan Leitner danken, mit denen mich viele wunderbare Erinnerungen verbinden.

Mein größter Dank gilt meiner Familie, vor allem meinen Eltern, ohne deren Unterstützung ich niemals dieses Studium erfolgreich beenden hätte können.

Abstract

The Geological Strength Index (GSI) provides a method for estimating the rock mass properties by field observations. It was introduced to obtain reliable, but also easily determinable parameters to describe rock mass properties for e.g. the design of tunnels. With the GSI it is also possible to calculate a block volume dependant Young's modulus for the rock mass, by using a closed form solution. However, the GSI relies strongly on subjective assumptions and therefore requires a reasonable work experience. When the GSI is calculated even small changes in the input values can have a significant effect on the results, for example the Young's modulus for rock masses (E_{RM}).

For a better estimation of the Young's modulus for rock mass (E_{RM}) a numerical model using a 3-dimensional distinct element code (3DEC) was applied to simulate jointed rock mass. The model is generated by applying rock material parameters to a block and splitting it with joints. It simulates a uniaxial compression test to obtain a stress-strain curve, which allows the determination of E_{RM} .

The model is split by one to three joint sets and variations in the spacing, persistence and the orientation of the joint sets are examined. For each of this variations the numerical and the empirical E_{RM} is compared. The results of the comparisons are analysed and interpreted.

Kurzfassung

Der Geological Strength Index (GSI) ist eine Methode zur Einschätzung der Gebirgseigenschaften durch Feldbeobachtungen. Er wurde eingeführt, um zuverlässige und dennoch einfach bestimmbare Parameter für Gebirgseigenschaften zu erhalten, welche für numerische Analysen weiterverwendet werden können (z.B. Tunneldesign). Mit dem GSI ist es auch möglich, einen blockvolumenabhängigen Steifigkeitsmodul für ein Gebirge mittels geschlossener Lösung zu berechnen. Die Verwendung des GSI ist jedoch sehr subjektiv und erfordert einige Berufserfahrung um korrekt angewandt zu werden. Wenn der GSI rechnerisch ermittelt wird, haben selbst kleine Änderungen bei den Eingangswerten einen erheblichen Einfluss auf die Ergebnisse wie z.B. bei der Berechnung des E-Moduls des Gebirges (E_{RM}).

Um den E-Modul des Gebirges (E_{RM}) besser abschätzen zu können, wurde mittels eines 3-dimensionalen distinct element Codes (3DEC) ein numerisches Modell eines klüftigen Gebirges erstellt. Mit dem Modell wird ein einaxialer Druckversuch simuliert, um eine Spannungs-Dehnungskurve zu erhalten, welche die Bestimmung des E_{RM} ermöglicht.

Das Modell wird von bis zu drei Trennflächenscharen zerteilt und es werden verschiedene Variationen der Orientierung, der Persistenz sowie des Abstands dieser Trennflächenscharen untersucht. Für jede dieser Variationen wird der numerische und der analytische E_{RM} miteinander verglichen. Die Ergebnisse dieser Vergleiche werden weiters analysiert und interpretiert.

Table of contents

1	Introduction	1
2	Objectives	2
3	State of the art	3
3.1	Hoek-Brown failure criterion	3
3.1.1	Petrographic constant / Material constant m_i	3
3.1.2	Disturbance Factor D	5
3.1.3	Mohr-Coulomb failure criterion	7
3.2	Hoek Chart.....	9
3.3	Quantified chart by Cai et al.	11
3.3.1	Block Volume V_b	12
3.3.2	Joint Condition Factor J_c	13
3.3.1	Estimation of the GSI with V_b and J_c	14
3.4	Chart with the latest quantification and application guidelines by Hoek	16
3.5	Estimation of the Young's modulus	18
4	Methodology	22
4.1	Numerical Simulation – 3DEC	22
4.1.1	General settings	22
4.1.2	Investigated cases.....	24
4.1.2.1	<i>Influence of V_b and the block shape</i>	24
4.1.2.2	<i>Influence of the persistence</i>	26
4.1.2.3	<i>Influence of other parameters</i>	26
4.1.3	Material and joint parameters	26
4.2	Evaluation of E_{RM}	28
4.2.1	GSI calculation	28
4.2.2	Sandwich Modell	29
4.3	Evaluation	30
5	Results	33
5.1	Influence of V_b and the block shape	33
5.1.1	Whole Block	33
5.1.2	Sandwich.....	34
5.1.3	Vertical Sandwich.....	35

5.1.4	Column.....	36
5.1.5	Beam.....	37
5.1.6	Three joint sets (3JS)	38
5.2	Influence of the persistence.....	40
5.3	Influence of other parameters.....	42
5.3.1	Joint normal stiffness.....	42
5.3.2	Influence of inclined of joints	42
6	Interpretation and Discussion	44
6.1	Influence of V_b	44
6.1.1	Block shapes.....	44
6.1.1.1	<i>Cubic shaped</i>	44
6.1.1.2	<i>Columnar shaped</i>	45
6.1.1.3	<i>Plate shaped</i>	46
6.1.1.4	<i>Beam shaped</i>	46
6.1.1.5	<i>Slab shaped</i>	47
6.1.2	Influence of the block shape	48
6.1.3	Impact of the joint spacing	49
6.1.4	“Plate Problem”	51
6.2	Influence of the persistence.....	53
7	Conclusion and Outlook	55
8	References	56
9	Internet bibliography	58
10	Appendix A	I

List of figures

Figure 1 Influence of the blast damage factor D on the rock mass strength (assuming $m_i = 20$) (left) and Influence of the blast damage factor D on the rock mass deformation modulus (right) [10]	5
Figure 2 Guidelines for estimating disturbance factor D [10]	6
Figure 3 Failure envelope of the Hoek-Brown criterion.....	8
Figure 4: Relationship between major and minor principal stresses for Hoek-Brown and equivalent Mohr-Coulomb criterion [5]	8
Figure 5 Original chart of the geological strength index.....	9
Figure 6 GSI for heterogeneous rock masses like flysch [13].....	10
Figure 7 GSI chart quantified by V_b and J_c [14].....	11
Figure 8 Block delimited by three joint sets	12
Figure 9 Two-dimensional GSI system visualization [16]	15
Figure 10 GSI chart quantified with RQD and modified lines [17].....	16
Figure 11 Scale dependant limitation of the application of the GSI [17].....	17
Figure 12 Relationship between GSI, intact rock strength (σ_i) and in situ modulus of deformation E_{RM} for $\sigma_i=100$ [1]	19
Figure 13 Measured rock mass modulus of deformation against GSI for Chinese and Taiwanese data [21]	20
Figure 14 Plot of Simplified Hoek and Diederichs equation for Chinese and Taiwanese data [21]	20
Figure 15 Plot of normalized in situ rock mass deformation modulus from China and Taiwan against Hoek and Diederichs equation.....	21
Figure 16 Velocity applied to the model	23
Figure 17 Sketch for a) cube b) column c) plate d) beam e) slab	25
Figure 18 Calculation of the deformation modulus of a jointed model [24].....	29
Figure 19 Total force applied to the model	30
Figure 20 Exemplary displacements of the model.....	31
Figure 21 Exemplary stress-strain diagram.....	32

Figure 22 "Whole Block" model a) blocks b) Contour of Displacement.....	33
Figure 23 "Sandwich" model a) blocks b) Contour of Displacement	34
Figure 24 "Vertical Sandwich" model a) blocks b) Contour of Displacement	35
Figure 25 "Column" model a) blocks b) Contour of Displacement	36
Figure 26 "Beam" model a) blocks b) Contour of Displacement	37
Figure 27 "3JS" model a) blocks b) Contour of Displacement	38
Figure 28 Block Volume and correlation of the E_{RM}	39
Figure 29 Block Volume and correlation of the E_{RM} in logarithmic scale	39
Figure 30 Block with a persistence of a) 0.3 and b) 0.8.....	40
Figure 31 V_b according to the persistence of the joint sets in logarithmic scale	40
Figure 32 E_{RM} in relation to the persistence	41
Figure 33 Impact of the joint normal stiffness j_{kn} on the $E_{RM,3DEC}$	42
Figure 34 Dip angle polar diagram.....	43
Figure 35 Comparison of the $E_{RM,3DEC}$ [GPa] with the $E_{RM,GSI}$ [GPa] for cubes	45
Figure 36 Comparison of the $E_{RM,3DEC}$ [GPa] with the $E_{RM,GSI}$ [GPa] for columns.....	45
Figure 37 Comparison of the $E_{RM,3DEC}$ [GPa] with the $E_{RM,GSI}$ [GPa] for plates	46
Figure 38 Comparison of the $E_{RM,3DEC}$ [GPa] with the $E_{RM,GSI}$ [GPa] for beams	47
Figure 39 Comparison of the $E_{RM,3DEC}$ [GPa] with the $E_{RM,GSI}$ [GPa] for slabs	47
Figure 40 $E_{RM,3DEC}$ for V_b $2,5 \cdot 10^6$ [cm ³] by shape in a box whisker plot	48
Figure 41 E_{RM} for V_b $2,5 \cdot 10^6$ [cm ³].....	49
Figure 42 Exemplary a) model and b) contour of the z-displacement for the "plate problem"	51
Figure 43 $E_{RM,3DEC}$ for the "median average spacing", the dashed lines indicate the fitted trend lines.....	54

List of tables

Table 1 Constant m_i for intact rock, by rock group [6].....	4
Table 2 Terms to describe large-scale waviness.....	13
Table 3 Terms to describe small-scale smoothness.....	13
Table 4 Rating for the joint alteration factor J_A	14
Table 5 Applied Velocity	24
Table 6 Definition of the shapes for orthogonal joint sets , with $x \leq y$	25
Table 7 Material Parameters.....	26
Table 8 Default parameters for the joint properties	27
Table 9 Joint Condition Values for the empirical calculation of $E_{RM,GSI}$	28
Table 10 Comparison of the resulting rock parameters for “Sandwich”	34
Table 11 Comparison of the resulting rock parameters for “Vertical Sandwich”.....	35
Table 12 Comparison of the resulting rock parameters for “Column”	36
Table 13 Comparison of the resulting rock parameters for “Beam”	37
Table 14 Comparison of the resulting rock parameters for “3JS”	38
Table 15 $E_{RM,3DEC}$ for $V_b = 2,5 \cdot 10^6$ [cm ³]	50
Table 16 List of E_{RM} [GPa] for "Plate" Problems with the corresponding spacing of the joint sets in [cm]	52
Table 17 List of the persistence with correlating $E_{RM,3DEC}$ and the reference spacing (sp_{ref}).....	54

Abbreviations

GSI	Geological Strength Index
RMR	Rock Mass Rating
RQD	Rock Quality Designation
RMi	Rock Mass Index
jkn.....	Joint Normal Stiffness
jks	Joint Shear Stiffness
E_{RM}	Young's Modulus for Rock Masses
$E_{RM,3DEC}$	Young's Modulus for Rock Masses calculated with 3DEC
$E_{RM,GSI}$	Young's Modulus for Rock Masses calculated with analytical method
E_G	Young's Modulus for Rock Masses calculated with the "Sandwich" method
V_b	Block Volume
J_C	Joint Condition Factor
J_A	Joint Alteration Factor
J_W	Rating for waviness
J_S	Rating for smoothness
σ_1	major effective principal stresses at failure
σ_3	minor effective principal stresses at failure
σ_{ci}	uniaxial compressive strength of the intact rock material
sp1.....	uniaxial compressive strength of the intact rock material
sp2.....	uniaxial compressive strength of the intact rock material
sp3.....	uniaxial compressive strength of the intact rock material
sp _{ref}	uniaxial compressive strength of the intact rock material

1 Introduction

The Geological Strength Index (GSI) is a method for assessing the reduction in rock mass strength by field observations and the geological conditions of the rock mass. It was developed by Hoek and Brown [1] as an advancement of the parameters of the Hoek-Brown failure criterion. Therefore, it is part of the method used to estimate the rock mass strength. The GSI is also used to estimate the Young's Modulus for Rock Masses (E_{RM}), which makes it an important and widely used parameter in rock mechanics. The advantage of the GSI is the easy determination of relatively reliable descriptive parameters for rock mass properties, which can be used for example for numerical and analytical analyses for the designing of tunnels.

Usually, the GSI is determined by the use of a chart [1]. This chart is based on the structure of the rock mass in question and the surface quality of the discontinuities. These parameters are obtained by the responsible geologist or geotechnical engineer and are therefore subjective and heavily depending on the experience of the engineer as well as the accessibility of the rock mass. Another considerable disadvantage of the current handling of the GSI is its application of V_b to determine E_{RM} [2]. However, the orientation of the intersecting joints to the main direction of loading and the resulting block shape is not considered. This can lead to the situation of different blocks with the same volume, but with different shapes, generating the same GSI but may show totally different deformations under loading conditions. Furthermore, all provided approaches so far only consider the rock mass as a two dimensional model and neglect the interferences of blocks along the third dimension. The values determined with the use of the GSI are also based on the experience from years of rock engineering, yet they are seldom validated by actual results.

For this master thesis, a three-dimensional numerical model was created in 3DEC to calculate the Young's modulus of the rock mass ($E_{RM,3DEC}$) and compared to the Young's modulus determined with the GSI ($E_{RM,GSI}$). The model consists of a block subdivided by joints and hence simulates a blocky rock mass. The program used for the model is 3D Distinct Element Code (3DEC) by Itasca Consulting Group Inc. This program is able to vary the joints in their orientation, strength, spacing, persistence, normal stiffness and shear stiffness. The goal of this master thesis is to compare the analytical determination of the GSI and its correlating E_{RM} with the here presented numerically method. With this an evaluation of the parameters is possible.

2 Objectives

According to the mentioned problem of the unclear influence of the block shape, the block volume and the actual deformation behaviour of a blocky rock mass, the elaboration of this thesis is oriented along the following questions:

- Is it possible to simulate a uniaxial compression test by the use of 3DEC and is the resulting E_{RM} similar to the E_{RM} that is empirically calculated by the use of the GSI?
- How is the numerical E_{RM} influenced by the block size, block volume, material parameters, j_{ks} , j_{kn} and the joint persistence?
- What are the limitations of the numerical model in the sense of the model size, proportion of the spacing and the persistence of the joints?

3 State of the art

3.1 Hoek-Brown failure criterion

The Generalized Hoek-Brown failure criterion was first introduced in 1980 [3] to obtain input data for design analyses for underground excavations in hard rock. The criterion started with the properties of intact rock and was subsequently expanded with options to reduce the intact rock properties on the basis of the characteristics of joints in a rock mass [1]. The goal was the combination of available rock mass classification schemes with geological observations, like the Rock Mass Rating (RMR) system [4].

Nowadays, the criterion is widely used and well established, largely due to the fact that there are few alternatives. [5].

The generalized form of the criterion is as follows:

$$\sigma_1 = \sigma_3 + \sigma_{ci} \left(m_b * \frac{\sigma_3}{\sigma_{ci}} + s \right)^a \quad \text{eq.1}$$

In addition to that, the parameters m_b , a and s are material constants which are defined as following:

$$m_b = m_i * \exp\left(\frac{GSI-100}{28-14D}\right) \quad \text{eq. 2}$$

$$s = \exp\left(\frac{GSI-100}{9-3D}\right) \quad \text{eq. 3}$$

$$a = \frac{1}{2} + \frac{1}{6} * \left(e^{-\frac{GSI}{5}} - e^{-\frac{20}{3}} \right) \quad \text{eq. 4}$$

As seen by these formulas, the original stress dependency is based on three parameters, the material constant for intact rock m_i , the disturbance factor D and the GSI. However, in the following years, the GSI experienced many adaptations and improvements, which are described in the following sections.

3.1.1 Petrographic constant / Material constant m_i

The material constant for intact rock (m_i) can be determined by using laboratory testing or estimating it with published data. The preferred method of determination should, if possible, always be by statistical analysis of the results of a set of triaxial tests on carefully prepared

core samples [1]. If such tests are not possible, the tables can be used for preliminary design purposes (e.g. Table 1). The material constant m_i is significantly different if failure occurs along a weakness plane.

The table for the determination of the m_i (Table 1) is divided into a number of sub-groups. At first the table is separated into rock types (igneous, metamorphic and sedimentary rocks), then into rock classes (clastic, non-clastic...), and finally into texture. The texture is divided into coarse, medium, fine and very fine.

Table 1 Constant m_i for intact rock, by rock group [6]

Rock type	Class	Group	Texture			
			Coarse	Medium	Fine	Very fine
SEDIMENTARY	Clastic		Conglomerate (22)	Sandstone 19 —— Greywacke —— (18)	Siltstone 9	Claystone 4
		Non-Clastic	Organic		Chalk 7 —— Coal —— (8-21)	
	Carbonate		Breccia (20)	Sparitic Limestone (10)	Micritic Limestone 8	
		Chemical		Gypstone 16	Anhydrite 13	
METAMORPHIC	Non Foliated		Marble 9	Hornfels (19)	Quartzite 24	
	Slightly foliated		Migmatite (30)	Amphibolite 25 - 31	Mylonites (6)	
	Foliated*		Gneiss 33	Schists 4 - 8	Phyllites (10)	Slate 9
IGNEOUS	Light		Granite 33		Rhyolite (16)	Obsidian (19)
			Granodiorite (30)		Dacite (17)	
	Dark		Diorite (28)		Andesite 19	
		Gabbro 27	Dolerite (19)	Basalt (17)		
		Norite 22				
	Extrusive pyroclastic type		Agglomerate (20)	Breccia (18)	Tuff (15)	

3.1.2 Disturbance Factor D

The disturbance factor D was introduced to include the subjects of blast damage and stress relaxation. With it, the effects of heavy blast damage as well as stress relief due to excavation, which results in a disturbance of the rock mass, are included into the GSI in 2002 [7]. It ranges from 0, which represents undisturbed in situ rock masses to 1, which represents very disturbed rock masses [5].

It was introduced due to the fact that in the design of slopes in very large open pit mines the Hoek-Brown criterion for undisturbed in situ rock masses ($D = 0$) results in rock mass properties that are too optimistic. [5,8]

A number of slope failures in Turkish open pit coal mines have been back-analysed to assign disturbance factors to each rock mass based upon their assessment of the rock mass properties predicted by the Hoek-Brown criterion [9].

Based on these back-analyses, a set of guidelines [5] has been developed, which can be used to estimate D (Figure 2). However, these guidelines have to be used with caution as the influence of the disturbance factor can be quite large. This can be seen very well in Figure 1

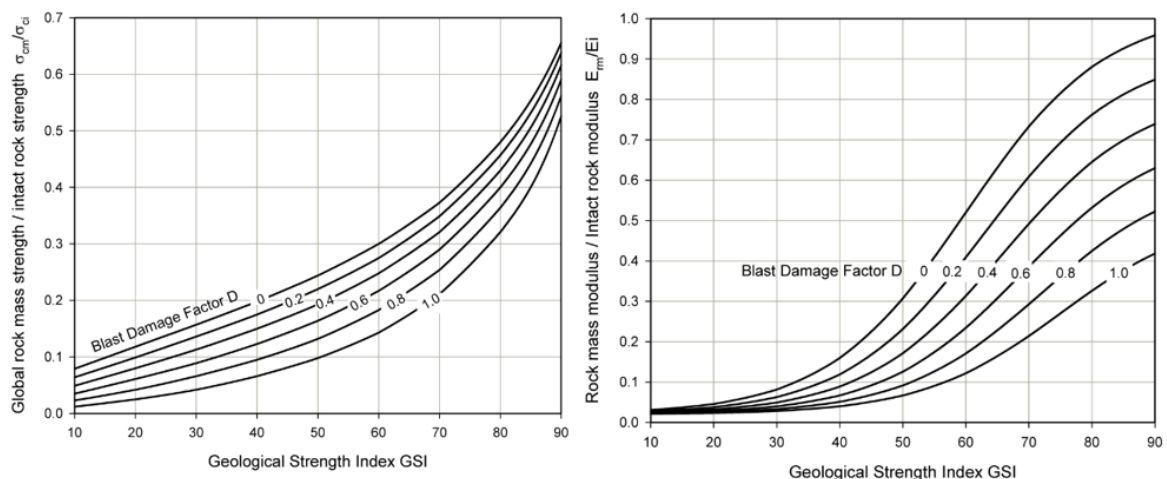


Figure 1 Influence of the blast damage factor D on the rock mass strength (assuming $m_i = 20$) (left) and Influence of the blast damage factor D on the rock mass deformation modulus (right) [10]

The main issues for applying D are choosing an appropriate value for the blast damage factor and the definition of the damaged zone. Figure 2, describes the main guidelines for the selection of D. [10].




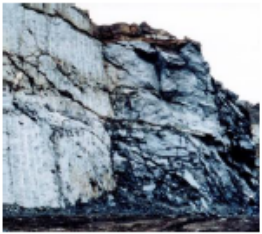

Appearance of rock mass	Description of rock mass	Suggested value of D
	Excellent quality controlled blasting or excavation by Tunnel Boring Machine results in minimal disturbance to the confined rock mass surrounding a tunnel.	$D = 0$
	Mechanical or hand excavation in poor quality rock masses (no blasting) results in minimal disturbance to the surrounding rock mass. Where squeezing problems result in significant floor heave, disturbance can be severe unless a temporary invert, as shown in the photograph, is placed.	$D = 0$ $D = 0.5$ No invert
	Very poor quality blasting in a hard rock tunnel results in severe local damage, extending 2 or 3 m, in the surrounding rock mass.	$D = 0.8$
	Small scale blasting in civil engineering slopes results in modest rock mass damage, particularly if controlled blasting is used as shown on the left hand side of the photograph. However, stress relief results in some disturbance.	$D = 0.7$ Good blasting $D = 1.0$ Poor blasting
	Very large open pit mine slopes suffer significant disturbance due to heavy production blasting and also due to stress relief from overburden removal. In some softer rocks excavation can be carried out by ripping and dozing and the degree of damage to the slopes is less.	$D = 1.0$ Production blasting $D = 0.7$ Mechanical excavation

Figure 2 Guidelines for estimating disturbance factor D [10]

3.1.3 Mohr-Coulomb failure criterion

The Hoek-Brown criterion is unlike the Mohr-Coulomb criterion not linear (Figure 3), therefore a conversion formula for an equivalent friction angle and cohesion had to be developed. This was achieved by fitting an average linear relationship to the curve generated by solving $\sigma_1 = \sigma_3 + \sigma_{ci} (m_b * \frac{\sigma_3}{\sigma_{ci}} + s)^a$ eq.1 for a range of minor principal stress values defined by $\sigma_t < \sigma_3 < \sigma'_{3max}$, this is shown in Figure 4.[5].

With this method the resulting equivalent friction angle is:

$$\varphi' = \sin^{-1} \left[\frac{6am_b(s+m_b\sigma'_{3n})^{a-1}}{2(1+a)(2+a)+6am_b(s+m_b\sigma'_{3n})^{a-1}} \right] \quad \text{eq. 5}$$

The resulting equivalent cohesion is:

$$c' = \frac{\sigma_{ci} * [(1+2a)s + (1-a)m_b\sigma'_{3n}] * (s+m_b\sigma'_{3n})^{a-1}}{(1+a)(2+a) \sqrt{1 + \frac{6am_b(s+m_b\sigma'_{3n})^{a-1}}{(1+a)(2+a)}}} \quad \text{eq. 6}$$

$$\text{With } \sigma_{3n} = \frac{\sigma'_{3max}}{\sigma_{ci}} \text{ and } \frac{\sigma'_{3max}}{\sigma_{cm}} = 0.47 * \left(\frac{\sigma'_{cm}}{\gamma H} \right)^{-0.94}$$

H is the depth below surface of a tunnel and γ is the unit weight of the rock mass. The rock mass strength σ'_{cm} is defined as

$$\sigma'_{cm} = \sigma_{ci} \frac{(m_b + 4s - a(m_b - 8s)) \left(\frac{m_b}{4+s} \right)^{a-1}}{2(1+a)(2+a)} \quad \text{eq. 7}$$

This conversion is necessary because the Mohr-Coulomb failure criterion is still widely used in geotechnical software, so this method was needed to make the Hoek-Brown criterion applicable to such software.

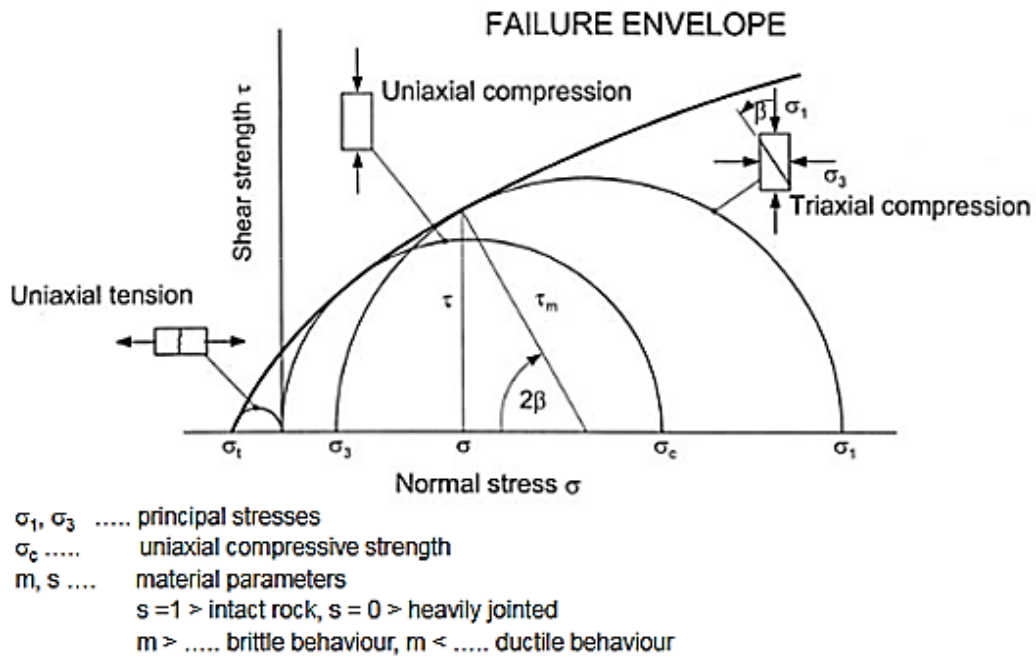


Figure 3 Failure envelope of the Hoek-Brown criterion

The comparison of the two criteria portrayed very good in Figure 4 **Error! Reference source not found.**

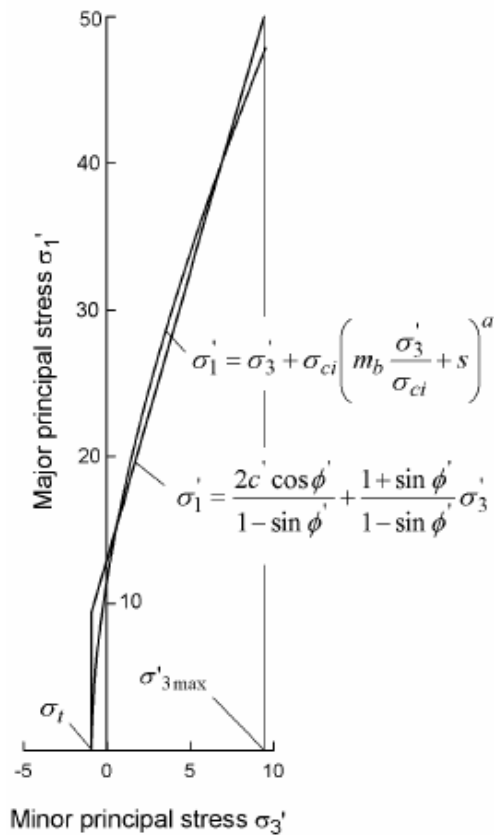


Figure 4: Relationship between major and minor principal stresses for Hoek-Brown and equivalent Mohr-Coulomb criterion [5]

3.2 Hoek Chart

The GSI was initially derived from the Rock Mass Rating (RMR) by Bieniawski [4] and the Q-System by Barton [11] to take the fundamental properties of a rock mass into account. Later, a method of direct determination was created based on a chart (Figure 5) . This chart summarized the qualitative assessment of the characteristics of the structure and the fracturing of the rock masses and their relative discontinuity characteristics. [1,12]

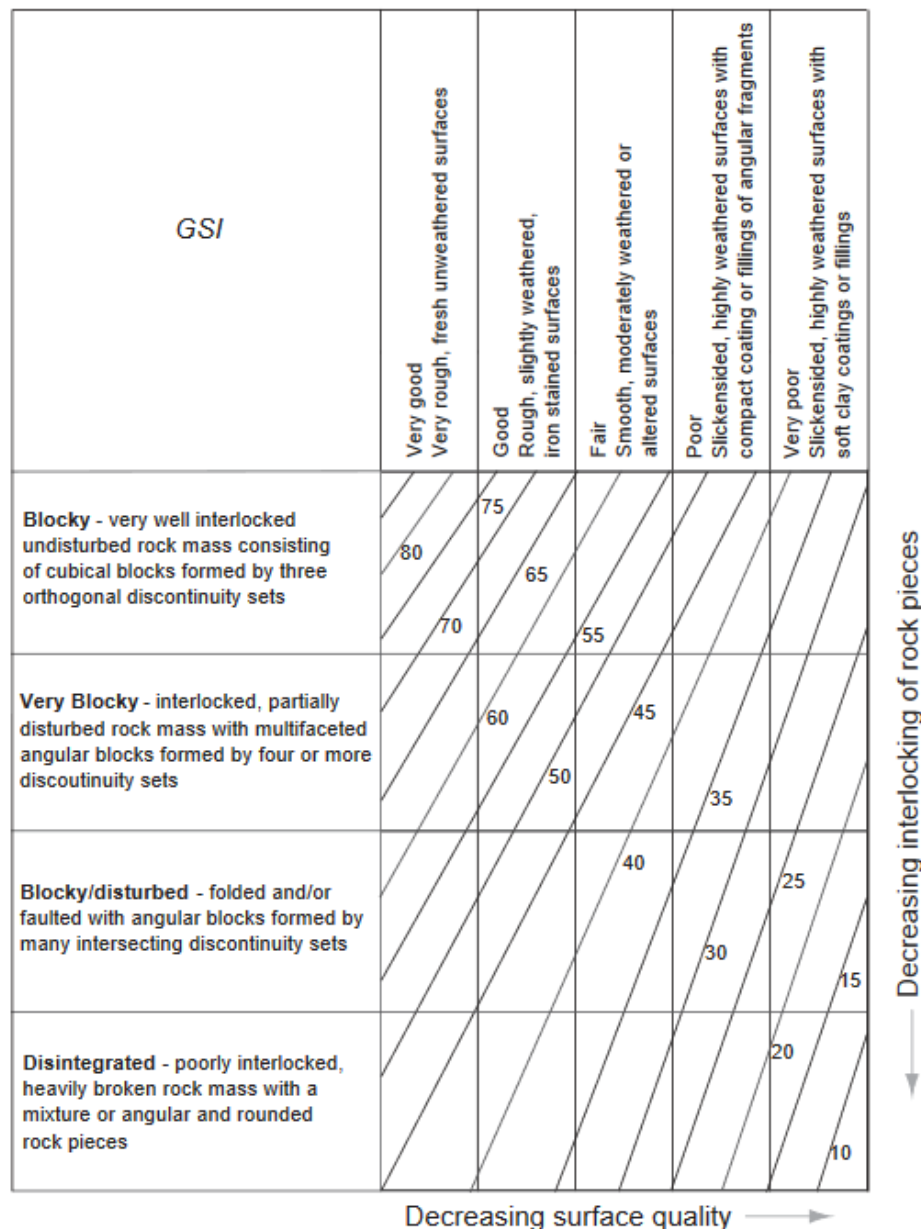


Figure 5 Original chart of the geological strength index

As an additional development, another diagram was created especially for obtaining a GSI for heterogeneous rock masses, e.g. flysch (Figure 6).

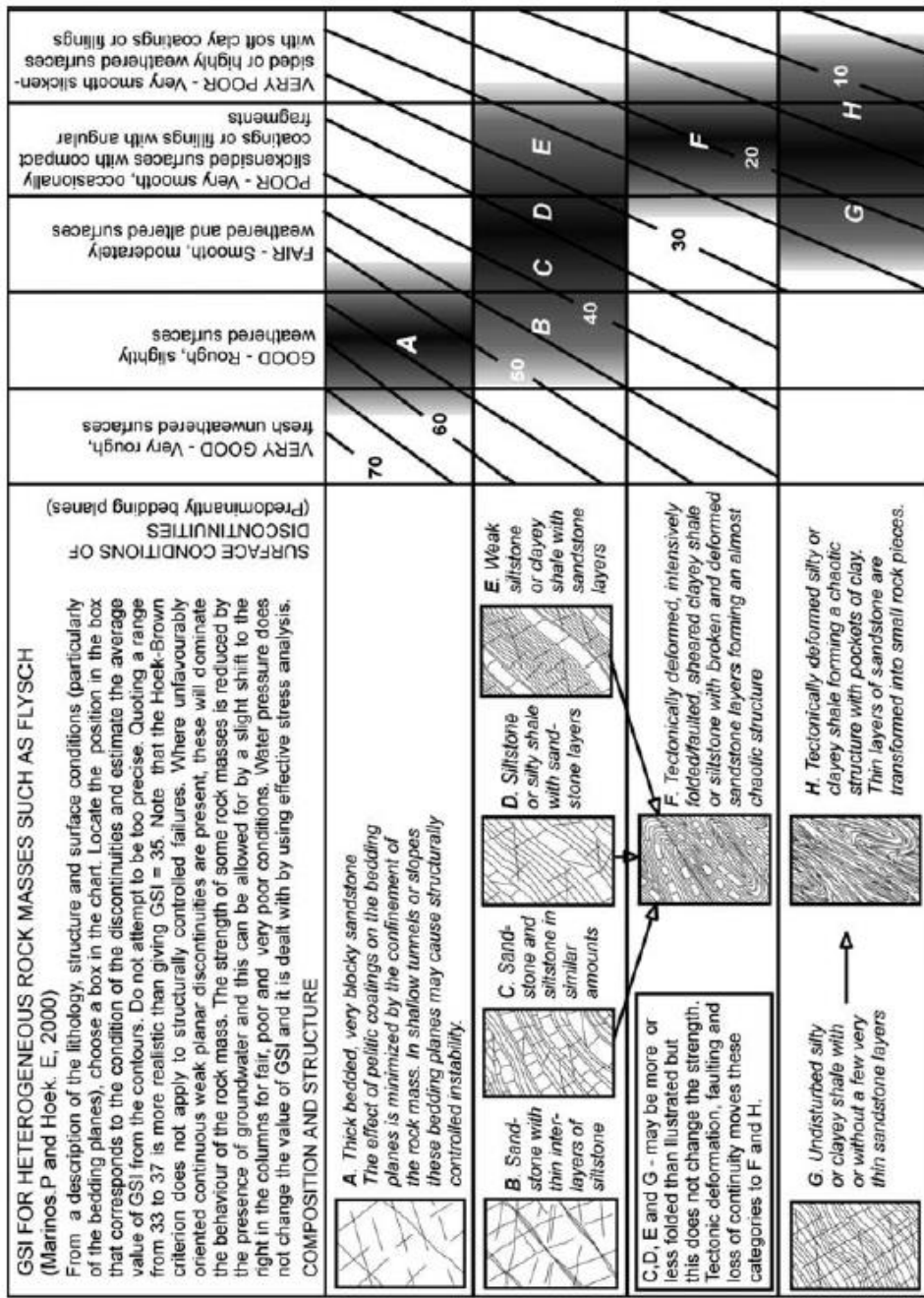


Figure 6 GSI for heterogeneous rock masses like flysch [13]

3.3 Quantified chart by Cai et al.

In 2004, Cai et al. developed a new chart, in which the GSI is estimated based on the block size and the joint surface condition (Figure 7). For this, the chart was quantified by the Joint Condition Factor (J_c) and by the Block Volume (V_b) [2], values which are measurable and quantitative. This leads to a reduced dependency of the determination of the GSI on experience while maintaining its relative simplicity. The original chart was also extended by two more structure categories. A row for massive, very interlocked and undisturbed rock mass blocks was added, as well as a row for foliated, laminated or sheared rock mass blocks.

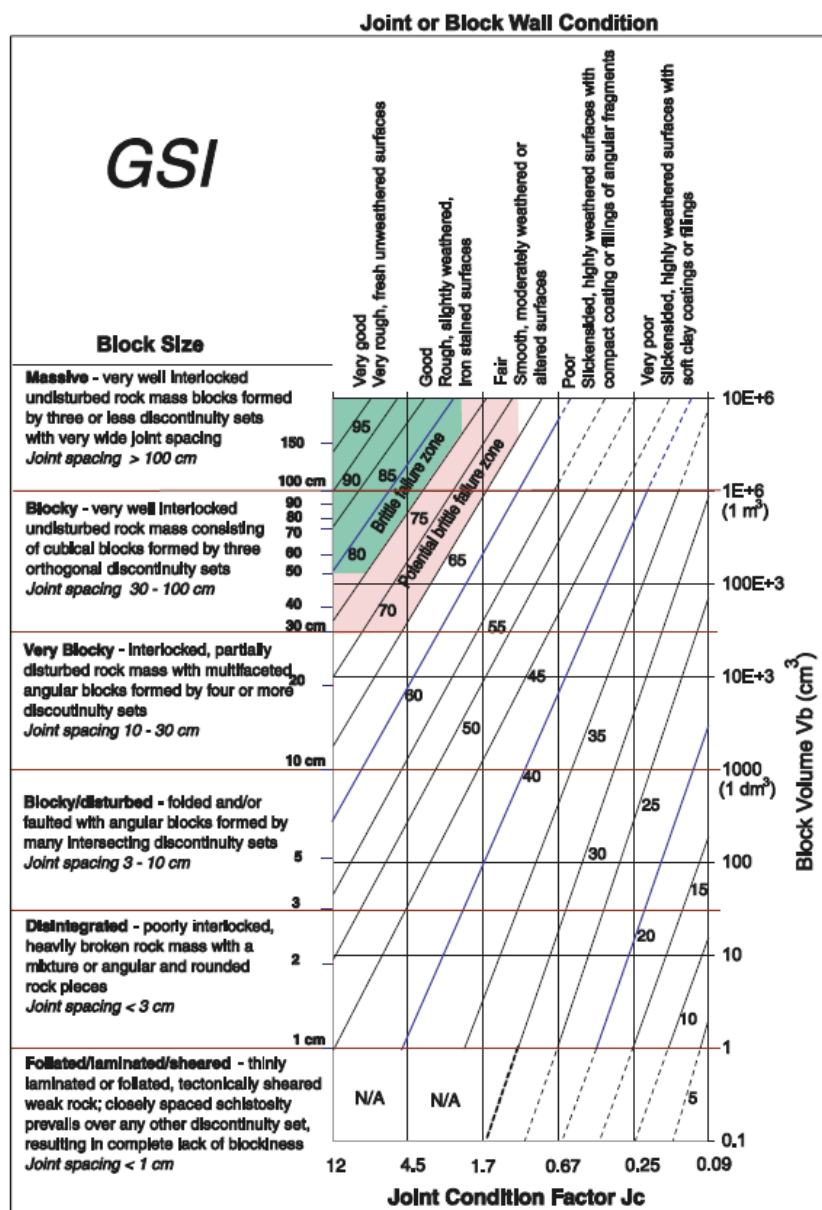


Figure 7 GSI chart quantified by V_b and J_c [14]

3.3.1 Block Volume V_b

V_b results from the spacing (s), intersection angles (γ), persistence (p) and the number of joint sets. It indicates the quality of rock masses and is a volumetric expression of joint density [15]. The lateral extent of joints is often limited, which is defined as the joint persistence. This persistence is important for the rock mass strength, for example if there are rock bridges and the joints are not persistent. This results in a higher rock mass strength and an improved global rock mass stability. To consider this effect, a concept of equivalent block volume was introduced which includes the persistence. The equivalent block volume is obtained by the following formula [2]:

$$V_b = \frac{s_1 s_2 s_3}{\sqrt[3]{p_1 p_2 p_3 \sin \gamma_1 \sin \gamma_2 \sin \gamma_3}} \quad \text{eq. 8}$$

Where γ_i is the angle between joint sets and s_i is the joint spacing. The joint persistence p_i is defined as follows

$$p_i = \begin{cases} \frac{\bar{l}_i}{L} & \bar{l}_i < L \\ 1 & \bar{l}_i \geq L \end{cases} \quad \text{eq. 9}$$

Where \bar{l}_i is the accumulated joint length of set i in the sampling plane and L is the characteristic length of the rock mass under consideration. [2]. This can be seen quite clear in Figure 8.

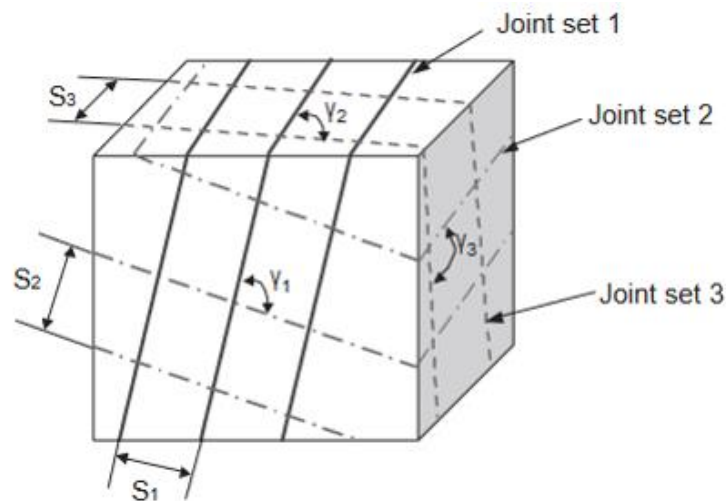


Figure 8 Block delimited by three joint sets

3.3.2 Joint Condition Factor J_C

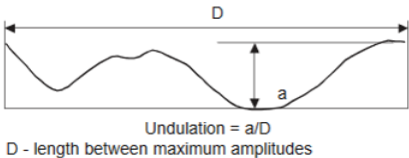
In the GSI system, the joint surface condition is defined by the roughness, weathering and infilling conditions. The combination of these factors defines the strength of a joint or block surface. The roughness is represented by the small-scale smoothness factor J_S , the weathering by the joint large-scale waviness factor J_W and the infill by the alteration factor J_A . The joint condition factor J_C is composed of these other factors and they are connected by the following formula:

$$J_C = \frac{J_W * J_S}{J_A} \quad \text{eq. 10}$$

The ratings are derived from the verbal descriptions of the Q-System and the Rmi and are listed in the following tables [2].

Table 2 Terms to describe large-scale waviness

Waviness terms	Undulation	Rating for waviness J_W
Interlocking (large-scale)		3
Stepped		2.5
Large undulation	> 3%	2
Small to moderate undulation	0.3–3%	1.5
Planar	<0.3%	1



Undulation = a/D
D - length between maximum amplitudes

Table 3 Terms to describe small-scale smoothness

Smoothness terms	Description	Rating for smoothness J_S
Very rough	Near vertical steps and ridges occur with interlocking effect on the joint surface	3
Rough	Some ridge and side-angle are evident; asperities are clearly visible; discontinuity surface feels very abrasive (rougher than sandpaper grade 30)	2
Slightly rough	Asperities on the discontinuity surfaces are distinguishable and can be felt (like sandpaper grade 30–300)	1.5
Smooth	Surface appear smooth and feels so to touch (smoother than sandpaper grade 300)	1
Polished	Visual evidence of polishing exists. This is often seen in coating of chlorite and specially talc	0.75
Slickensided	Polished and striated surface that results from sliding along a fault surface or other movement surface	0.6–1.5

Table 4 Rating for the joint alteration factor J_A

	Term	Description	J_A
Rock wall contact	<i>Clear joints</i>		
	Healed or "welded" joints (unweathered)	Softening, impermeable filling (quartz, epidote, etc.)	0.75
	Fresh rock walls (unweathered)	No coating or filling on joint surface, except for staining	1
	Alteration of joint wall: slightly to moderately weathered	The joint surface exhibits one class higher alteration than the rock	2
	Alteration of joint wall: highly weathered	The joint surface exhibits two classes higher alteration than the rock	4
	<i>Coating or thin filling</i>		
	Sand, silt, calcite, etc.	Coating of frictional material without clay	3
Filled joints with partial or no contact between the rock wall surfaces	Clay, chlorite, talc, etc.	Coating of softening and cohesive minerals	4
	Sand, silt, calcite, etc.	Filling of frictional material without clay	4
	Compacted clay materials	"Hard" filling of softening and cohesive materials	6
	Soft clay materials	Medium to low over-consolidation of filling	8
	Swelling clay materials	Filling material exhibits swelling properties	8-12

According to equation 10 and Table 4, J_A is the factor with the most impact and has therefore to be the one chosen with the most precaution.

3.3.1 Estimation of the GSI with V_b and J_C

With a quantitative chart and surface fitting systems, a formula was created to show the relationship between the parameters of the new chart, J_C and V_b , and the GSI [14] .

$$GSI(V_b, J_C) = \frac{26.5 + 8.79 \cdot \ln J_C + 0.9 \cdot \ln V_b}{1 + 0.0151 \cdot \ln J_C - 0.0253 \cdot \ln V_b} \quad \text{eq. 11}$$

Where J_C has no dimension and V_b is expressed in cm^3 [16].

With this method, it was possible to produce a two-dimensional visualization in a log-log plot [16] (Figure 9). The GSI here is a function of two parameters $f=f(x_1, x_2)$ with x_1 being the V_b in cm^3 and x_2 being the J_C . According to this visualization, the GSI calculated with this method is limited by V_b and, at a very small volume (e.g. 0.1 cm^3), the GSI cannot become higher than 40 even at the best J_C .

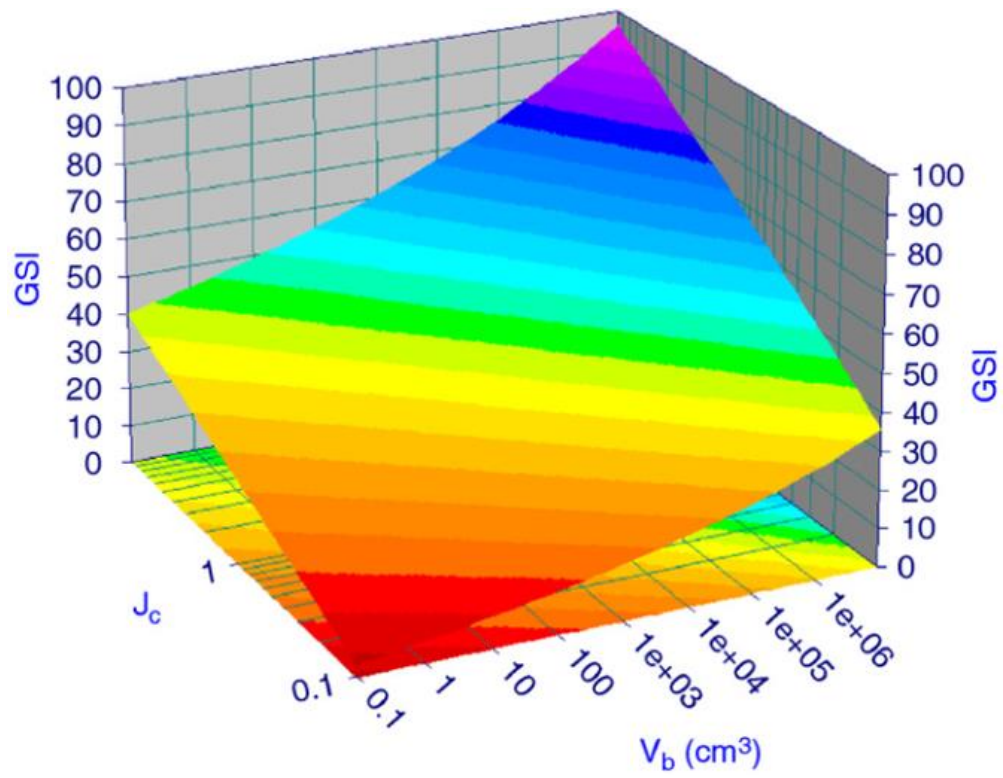


Figure 9 Two-dimensional GSI system visualization [16]

3.4 Chart with the latest quantification and application guidelines by Hoek

After several years of using the GSI, an evaluation by Hoek took place to improve it [17]. One improvement was the redrawing of the lines in the chart. In this evaluated chart they are parallel to each other and have a constant distance between each other, unlike the lines in the original chart, which were hand-drawn (Figure 10). Also a quantification has been added, similar to the one at the block volume depended chart. This chart uses the Rock Quality Designation (RQD) and the Joint Condition rating (JCond89) by Bieniawski [17]. In addition, the number of rows describing the structure was reduced to four by dropping the row for intact and massive rock and the row for laminated/sheared rock from the original chart.

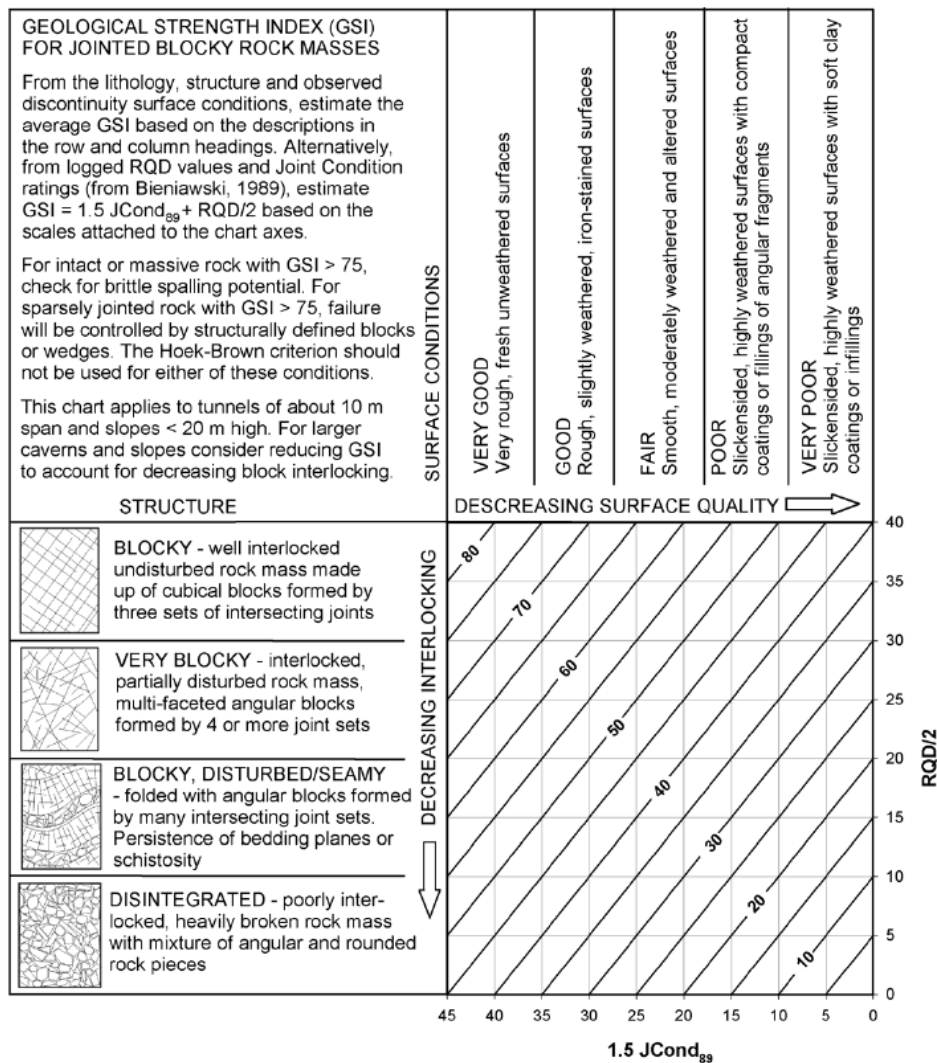


Figure 10 GSI chart quantified with RQD and modified lines [17]

Those two rows were removed due to the confusion they created when using the chart, as

they represented block structures for which the GSI is not suitable. The GSI chart as input parameters for the Hoek-Brown criterion should not be used for intact massive or very sparsely jointed rock, as shown in Figure 11. The reason for that is that there are insufficient pre-existing joints to satisfy the conditions of homogeneity and isotropy.

The Hoek-Brown criterion assumes that the peak strength and the deformation is governed by sliding and rotations of intact rock blocks defined by intersecting joint sets. This joint sets have to be sufficiently closely spaced, relative to the size of the structure under consideration, that the rock mass can be considered homogeneous and isotropic. This concept is illustrated in Figure 11. [17]

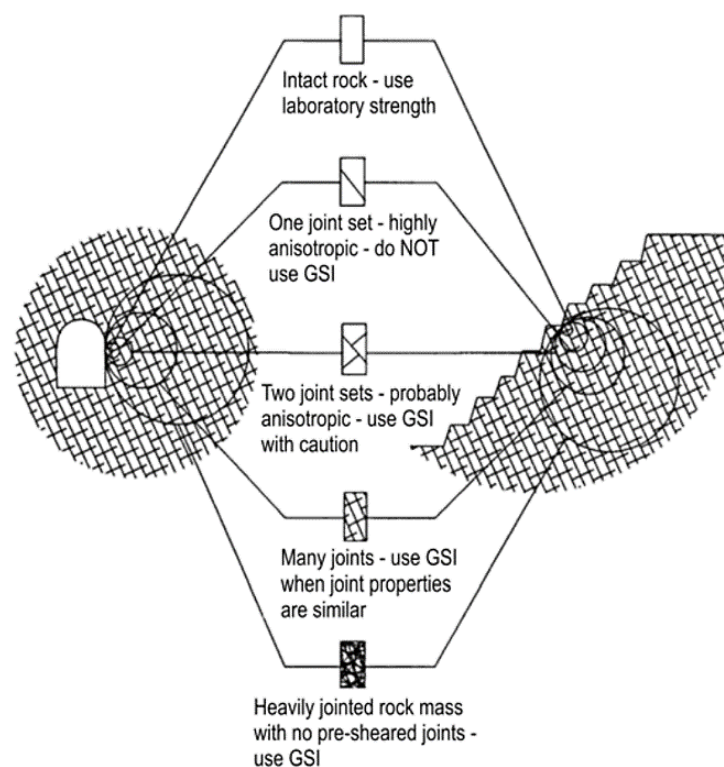


Figure 11 Scale dependant limitation of the application of the GSI [17]

3.5 Estimation of the Young's modulus

The Young's modulus for a rock mass (E_{RM}) is a very important parameter in numerical analyses. The determination of E_{RM} by field test is sometimes connected to quite high costs. Therefore, Bieniawski [18] developed a method to approximate E_{RM} , by using the RMR: This approximation is as following:

$$E_m = 2 \cdot RMR - 100 \quad \text{for } RMR > 50 \quad \text{eq. 12}$$

For cases when the RMR is less than 50 Serafim and Pereira [19] developed a different method:

$$E_m = 10^{\frac{RMR-10}{40}} \quad \text{for } RMR < 50 \quad \text{eq. 13}$$

With those established relationships Hoek [20] tried to connect the GSI with the determination for the E_{RM} , by assuming the RMR to be equal to the GSI for values larger than 25 ($GSI > 25$).

$$E_m = 2 \cdot GSI - 100 \quad [GPa] \quad \text{eq. 14}$$

$$E_m = 10^{\frac{GSI-10}{40}} \quad [GPa] \quad \text{eq. 15}$$

With the help of these formulas, the applicability of the GSI for weak and sheared rock masses was evaluated by back analysing a set of samples from the Athens Schist Formation. The experiences lead to the addition of the disturbance factor D into the formula and to the extension of the Hoek chart with a row for foliated/laminated/shear-structures. [1]. The new extended formula was:

$$E_m = \left(1 - \frac{D}{2}\right) * 10^{\frac{GSI-10}{40}} \quad [GPa] \quad \text{eq. 16}$$

Later, this formula was extended for cases when $\sigma_{ci} > 100$ MPa. [5] This extension lead to this equation:

$$E_m = \left(1 - \frac{D}{2}\right) * \sqrt{\frac{\sigma_{ci}}{100}} * 10^{\frac{GSI-10}{40}} \quad [GPa] \quad \text{eq. 17}$$

The relationship between the GSI and the deformation modulus that is created by this formula is illustrated in Figure 12.

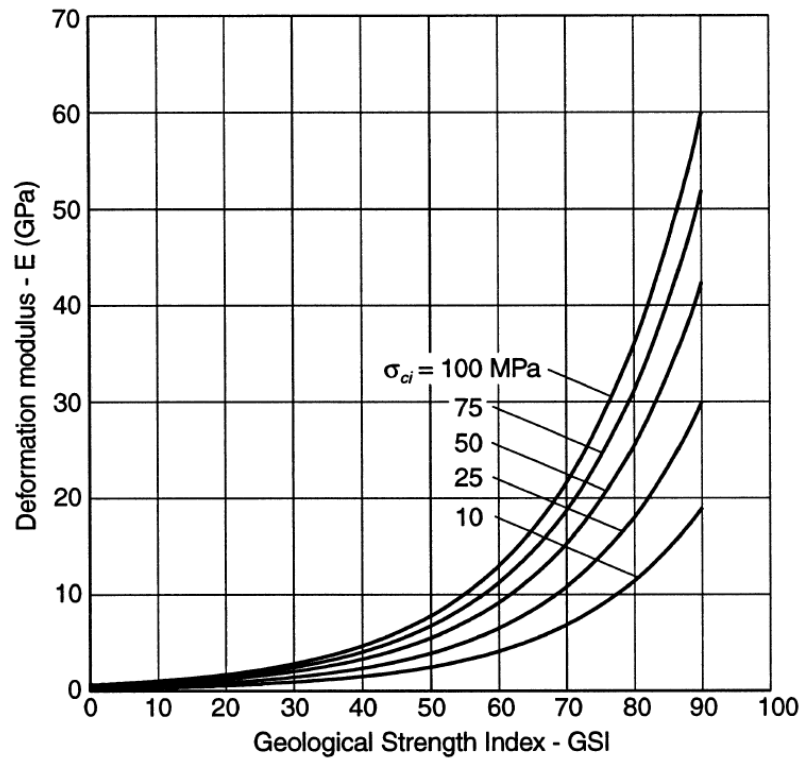


Figure 12 Relationship between GSI, intact rock strength (σ_i) and in situ modulus of deformation E_{RM} for $\sigma_i=100$ [1]

Due to the fact that in certain cases, when using this formula, it is possible that the resulting rock mass modulus is higher than the one for the intact rock, a new method had to be developed. For that an analysis of a large numbers of in-situ measurements from China and Taiwan was carried out (Figure 13). The data of insitu measurements was provided by Dr J.C. Chern of Taiwan. [21]

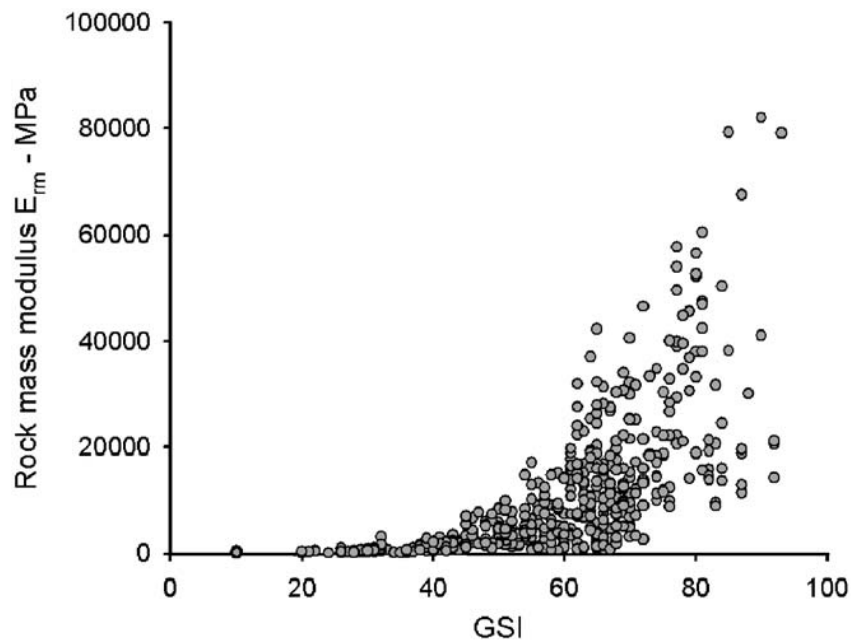


Figure 13 Measured rock mass modulus of deformation against GSI for Chinese and Taiwanese data [21]

To cap the increase of E_{RM} and therefore prevent an unrealistically high rock mass modulus, a sigmoidal function was used. In its general form, this S-shaped function is as following:

$$y = c + \frac{a}{1 + e^{\frac{x-x_0}{b}}} \quad \text{eq. 18}$$

The parameters y , a , b and c are variables for this generalized form of the equation.

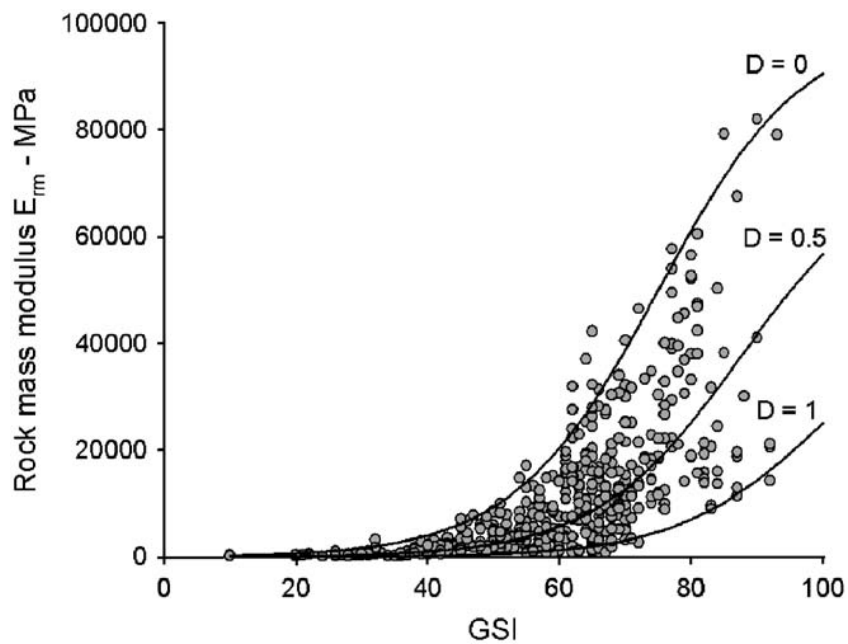


Figure 14 Plot of Simplified Hoek and Diederichs equation for Chinese and Taiwanese data [21]

By the use of a commercial curve fitting software this equation was fitted to the in situ data (Figure 13). This resulted in the following best-fit equation to determine the E_{RM} :

$$E_{rm} = E_i \left(0.02 + \frac{1 - \frac{D}{2}}{1 + e^{\frac{60 + 15D - GSI}{11}}} \right) \quad \text{eq. 19}$$

The resulting equation was plotted against the field data to show its accuracy. To summarize it better the average normalized field data were used (Figure 15).

When the E_i is not known, it can be estimated with the modulus ratio MR [22]. This ratio is:

$$E_i = MR \sigma_{ci} \quad \text{eq. 20}$$

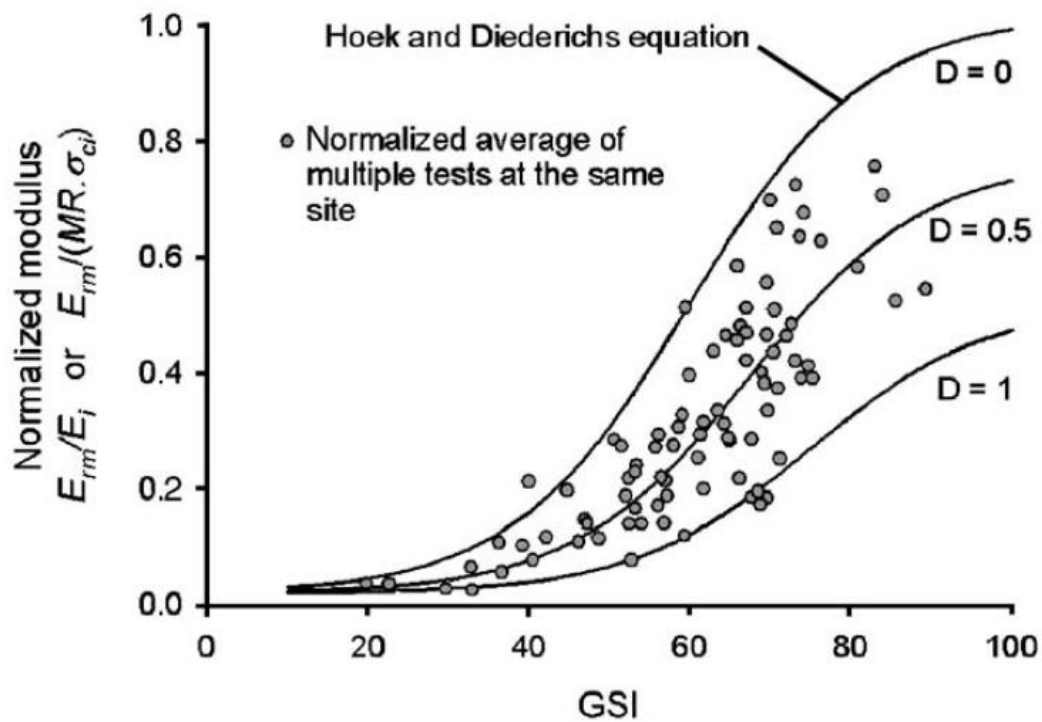


Figure 15 Plot of normalized in situ rock mass deformation modulus from China and Taiwan against Hoek and Diederichs equation.

4 Methodology

4.1 Numerical Simulation – 3DEC

3DEC is a three-dimensional numerical modelling code by the Itasca Consulting Group. It is used for advanced geotechnical analysis of soil, rock, ground water, structural support, and masonry. It is able to simulate the response of discontinuous media when static or dynamic loading is applied to them. The method is the distinct element method (DEM) for discontinuous modelling. (Itasca Consulting Group)

With this method the rock mass is described as an assemblage of discrete blocks, which are separated by discontinuities, in this master thesis defined as joints. With the DEM it is also possible to have large displacements along discontinuities, as well as the rotation of blocks. Based on the chosen constitutive and joint model the individual blocks can behave as either deformable or rigid material. It is also possible to generate continuous and discontinuous joint patterns, this is then based on statistics. (Itasca Consulting Group)

Similar to other Itasca products, like UDEC, 3DEC has the built-in scripting language FISH encoded. (Itasca Consulting Group)

4.1.1 General settings

For the model dimensions, a cubic block with an edge length of 10 meters was chosen, therefore the coordinates of the origin are (0,0,0), which is the lower left front-corner of the model. To this block joint sets are applied in order to simulate a discontinuous/blocky rock mass. The number, length of the spacing and persistence of these joints have been altered and varied as part of this master thesis. Due to the fact that 3DEC is a code based program, several data files have been created to easily work with the program. In general, a displacement controlled uniaxial compression test with loading on the top and bottom of the discontinuous block is modelled. The complete code can be found in the appendix (A).

In the “main”-file, all the variables and input parameters are defined with FISH variables. The code is structured in such a way, that for changing the model the variables have to be changed only in this “main”-file. All other commands, for example the “poly brick”-command, which creates the block, just use the newly defined variables. This ensures an efficient way to alter or modify the code. These parameters are the input values for the modelling, the loading, the material and the joints.

In the “load”-file the implementation of the predefined displacements is defined, since the model is path-controlled. For the investigations, an array with 17 load-steps is created. Due to the fact that 3DEC always adds new boundary conditions to the existing ones, it was necessary to redefine the predefined displacements within the code. Therefore, a side-calculation within 3DEC was generated that every subsequent displacement had to be the difference of the predefined displacement and the previous applied one. These newly defined displacements are then added iteratively. To simulate a uniaxial compression test, the load steps are applied on both the top and the bottom of the block, this is comparable to a load plate lowering by a predefined distance. The results are listed in Table 5 and chosen according to the rock mass strength and shall not exceed the linear elastic/ideal plastic material behaviour, unless it is explicitly desired.

By using a predefined intrinsic function of FISH, every grid point of the jointed block is associated with an index number and its reaction forces can be exported to an Excel sheet. By using another predefined intrinsic function, every block that is generated by jointing the model can be assigned an index number and the volumes of these blocks can be read out. These output data have been copied into MS Excel for further analysis.

Every single load step is cycled 1000 times which correlates with an approximated limit equilibrium within reasonable computation time. The number is derived empirically and preserves the stable state. If this approximation would not have been used the computation time for each model would have been increased significantly. When this number is increased or decreased reasonably, the E_{RM} is not effected.

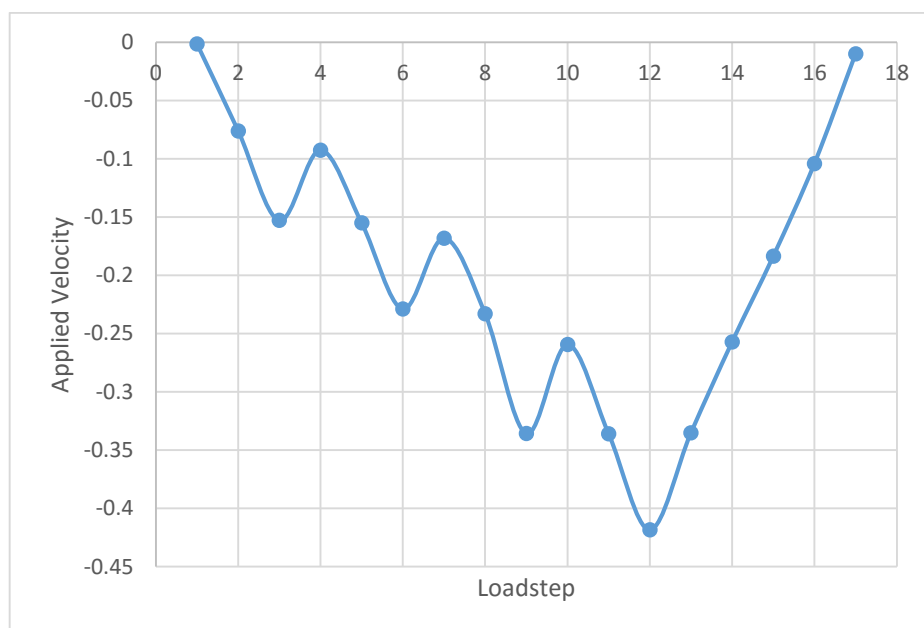


Figure 16 Velocity applied to the model

The input values of the displacements, which are applied on the boundaries of the model, are simulating a uniaxial compressive strength test. Similar to a real test, the deformation is applied on the upper and lower surface of the test sample. As can be seen in Table 5 there are 3 unloading steps, on the 4th, the 7th and the 10th load-step as well as a final unloading after the 12th load-step.

Table 5 Applied Velocity

Load-Steps	Applied Velocity	Load-Steps	Applied Velocity
1	-0.000144	10	-0.025954
2	-0.007603	11	-0.0336
3	-0.015292	12	-0.04185
4	-0.009251	13	-0.03353
5	-0.015513	14	-0.02572
6	-0.022904	15	-0.01837
7	-0.016812	16	-0.01041
8	-0.023295	17	-0.00099
9	-0.033592		

4.1.2 Investigated cases

The joint sets are defined by the dip angle, the dip direction, the number of joints per joint set, the spacing between the joints and the persistence of the joint.

4.1.2.1 Influence of V_b and the block shape

The spacing is the normal distance between the joints of each set, measured in meter. The number of joints is the quantity of joints that make up one set, this correlates with the spacing. The joints are produced symmetrically about the joint set origin. If the number multiplied with the spacing exceeds the model size, the joints that are unnecessary are not considered in the model. The spacing parameters also define the block volume and the shape of the blocks that are generated by splitting the model. The joint spacing in x-direction is named sp1, y-direction sp2 and z-direction sp3. It has to be noted that the displacements are applied in the z-axis. To determine the impact of the shape five types are defined.

For this definition, the spacing perpendicular to the load is defined as z , and the two in load

direction as x and y , but with the condition that $x \leq y$. This special labelling is because during the calculations of the models neither $sp1$ nor $sp2$ were defined as the smaller or larger one. With those boundary conditions the definitions for each shape are listed in Table 6. As those shapes all have corners with square angles

Table 6 Definition of the shapes for orthogonal joint sets , with $x \leq y$

Shape	x/z	y/z	x/y
Cube	= 1	= 1	= 1
Column	< 1	< 1	≤ 1
Plate	< 1	> 1	< 1
Slab	> 1	> 1	≤ 1
Beam	≤ 1	> 1	< 1

Exemplary sketches are illustrated in Figure 17. As can be seen the main differences between a column and a beam is the direction of the loading, otherwise a beam would just be a rotated column. The same applies to the difference between a plate and a slab.

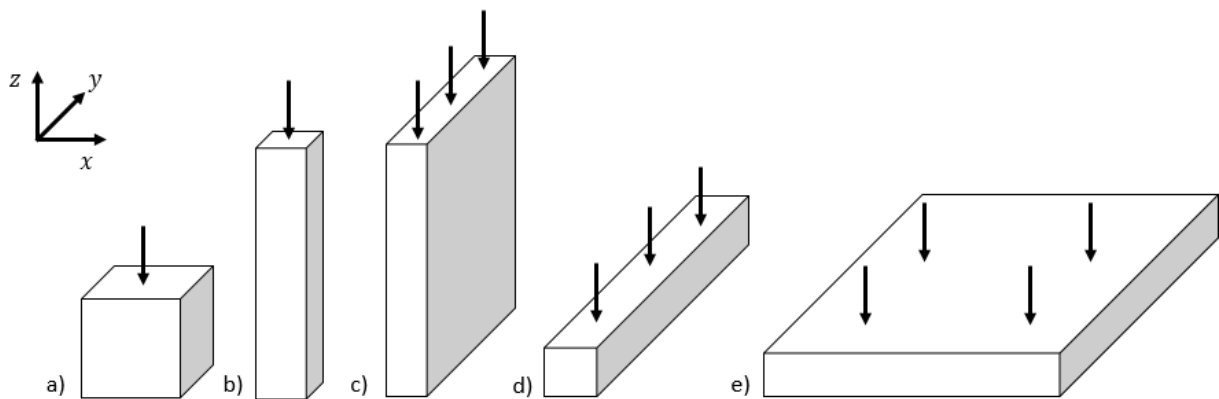


Figure 17 Sketch for a) cube b) column c) plate d) beam e) slab

The block shapes follow the classification of [23], however, this classification had to be adjusted according to the orientation of the load applied on the block.

4.1.2.2 Influence of the persistence

Joint bridges are created on a probabilistic basis. This implies that each new model with the same persistence can have different average block volumes. For evaluating the $E_{RM, GSI}$ the median block volume was chosen.

4.1.2.3 Influence of other parameters

The influence of the joint normal stiffness (jkn) was studied by altering the jkn for a number of models. The default model for this cases was a model with three joint sets orthogonal to each other.

To analyse the impact that the inclination has on the E_{RM} , the dip angle of the joint set perpendicular to the x-y plane was increased from 0° to 90° in steps of 2° to 5° . This is based on the assumption that as long as only one dip angle is modified, the effects on the model are the same as if the one perpendicular to the y-axis would be changed.

4.1.3 Material and joint parameters

The parameters set to define the material, for a massive rock (e.g. granite) are given in Table 7.

Table 7 Material Parameters

Material Parameters	Input value
Density	0.0027
Poisson's ratio [-]	0.25
Young's' modulus [MPa]	50'000
Cohesion [MPa]	15
dilatation angle [°]	0
friction angle [°]	30
tensile strength [MPa]	0.7
bulk modulus [MPa]	33'333.3
shear modulus [MPa]	20'000

For the joint parameters, a relatively high joint normal stiffness (jkn) and a relatively low joint shear stiffness (jks) have been chosen. The parameters are listed in

Table 8.

Table 8 Default parameters for the joint properties

Joint Parameters	Input value
Joint Normal Stiffness [MPa]	500'000
Joint Shear Stiffness [MPa]	5'000
Joint Friction Angle [°]	27
Joint Cohesion [MPa]	0

The constitutive model was set to be elastic/plastic with Mohr-Coulomb failure.

4.2 Evaluation of E_{RM}

4.2.1 GSI calculation

$E_{RM,GSI}$ is calculated according to eq. 19. The formula requires the determination of the block volume dependant GSI according to 11. However, the block volume (V_b) is not calculated with eq. 8 proposed by Cai et al. [2], but the exact V_b , internally calculated by 3DEC, using the median block volume of the jointed rock mass. This step increased the accuracy especially in models with no orthogonal discontinuity set.

For the joint condition factor (J_C), the joint waviness (J_W), the small scale roughness (J_S) and the joint alteration (J_A), three cases were considered, a so-called “best case”, a “worst case” and an “average case”. This had to be done because the J_C has a high impact on the GSI, but is very depended on the conditions of the joints of the actual rock mass, so these three cases were chosen to gain a fair representation for the many different possible joint conditions of each theoretical joint. The parameters chosen for the calculations are shown in Table 9. The input values are derived from the tables in chapter 3.3.2 and resemble the chosen material/joint properties of the calculations in 3DEC.

Table 9 Joint Condition Values for the empirical calculation of $E_{RM,GSI}$

Case	best case	worst case	average
Joint waviness (J_W)	2.55	1.75	2.15
Small Scale Roughness (J_S)	1	0.8	0.9
Joint Alteration (J_A)	1.5	8	4.75
Joint Condition (J_C)	1.7	0.175	0.407

According to the definitions from the Table 2, Table 3 and Table 4, the best case represents a joint that is interlocking to stepping/smooth and has a slightly weathered contact to the rock wall. The worst case represents a joint with a moderate undulation, it is polished to smooth and has joints filled with soft clay materials. The average case represents a joint which has a large undulation, is polished to smooth and has joints filled with a filling of frictional material without clay.

The chosen Young's modulus for intact rock E_i is set at 50 GPa. The disturbance factor D was set to 0. For all three cases from Table 9 a separate E_{RM} is calculated to compare it with the $E_{RM,3DEC}$.

4.2.2 Sandwich Modell

To have an additional comparison, models with only one joint set were also analysed with the following method for the empirical calculation of the Young's modulus for rock masses.

In this simplified model [24], a linear-elastic behaviour is assumed. For calculating the Young's modulus, the applied stress is divided by the total deformation. The thickness of the joints in proportion of the model length L is assumed to be insignificant. The deformation consists of two components, the deformation of intact rock Δu_i and the deformation of the joints Δu_T . These are defined as $\Delta u_i = \frac{\sigma L}{E}$ and $\Delta u_T = \frac{\sigma}{E_T}$.

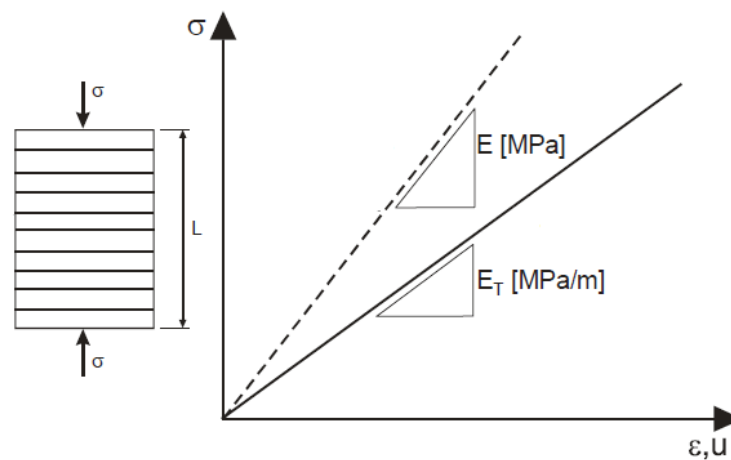


Figure 18 Calculation of the deformation modulus of a jointed model [24]

E_T is defined as the Young's modulus of joints per meter of the rock mass. The number of joints in the rock mass N is defined by a joint frequency λ . This frequency is the number of joints times the model length $\lambda = \frac{N}{L}$.

The deformation of the sum of those joints is defined as $\Delta u_T' = \frac{\sigma \lambda L}{E_T}$. Therefore the total deformation is $\Delta u_G = \frac{\sigma L}{E} + \frac{\lambda \sigma L}{E_T}$ and the total strain is calculated with:

$$\varepsilon = \frac{\Delta u_G}{L} = \frac{\sigma}{E} + \frac{\lambda \sigma}{E_T}. \quad \text{eq. 21}$$

As a result, the Young's modulus of the rock mass E_G is:

$$E_G = \frac{\sigma}{\varepsilon} = \frac{1}{\frac{1}{E} + \frac{\lambda}{E_T}} \quad \text{eq. 22}$$

4.3 Evaluation

The output file for further calculations consists of five columns. The first column lists the indexes of each grid-point associated with the matching boundary corner. The second column contains the displacements applied in z-direction at the boundary (bottom/top region). These displacements reflect the predefined input values. The third column lists the reaction forces in z-direction at the boundaries that are generated by applying the displacements. The next column consists of the dislocations of each grid point, that are generated as result of the applied displacements. These dislocations are not always the same as the applied displacements, because the model simulates a load plate lowering down on the top and the bottom, therefore the grid points closer to the centre do not dislocate exactly as the predefines displacements.

With that information, a total displacement of the loaded block can be calculated (Figure 20). The fifth column returns the reaction force in z-direction for a grid point that has been assigned a zero-velocity boundary condition. This step was just for control purpose as it results on zero, because the grid point is fixed. With the reaction forces in the z-direction, the total force for each load step can be calculated (Figure 19). From this, the stresses can be determined by dividing it with the surface area of the model (100 m²). All the output files for each model will be on a data storage device added to the thesis.

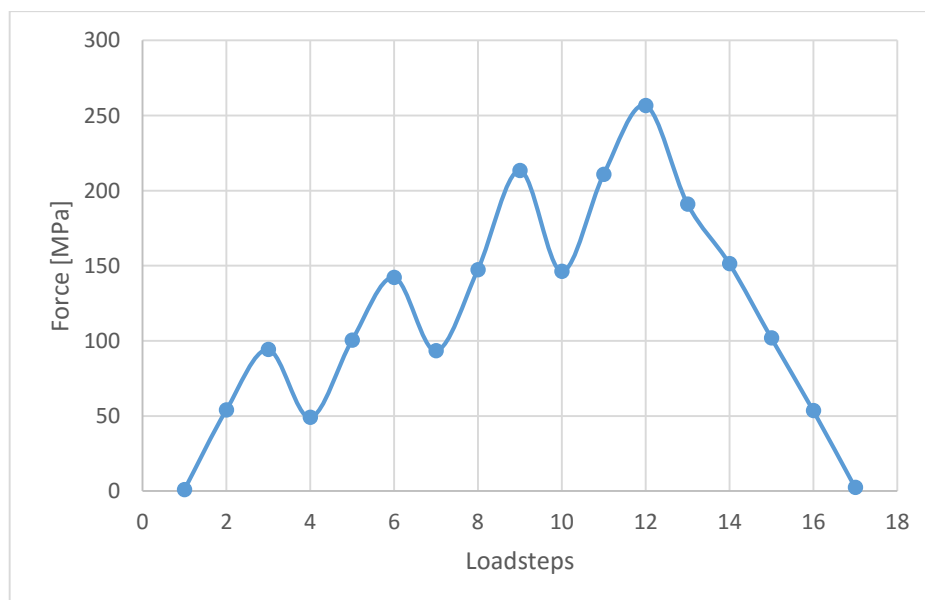


Figure 19 Total force applied to the model

The strains (ϵ) are calculated by summing up the displacements on the top and the bottom (Δl) and divided by the original height of the model (L)

$$\epsilon = \frac{\Delta l}{L} \quad \text{eq. 23}$$

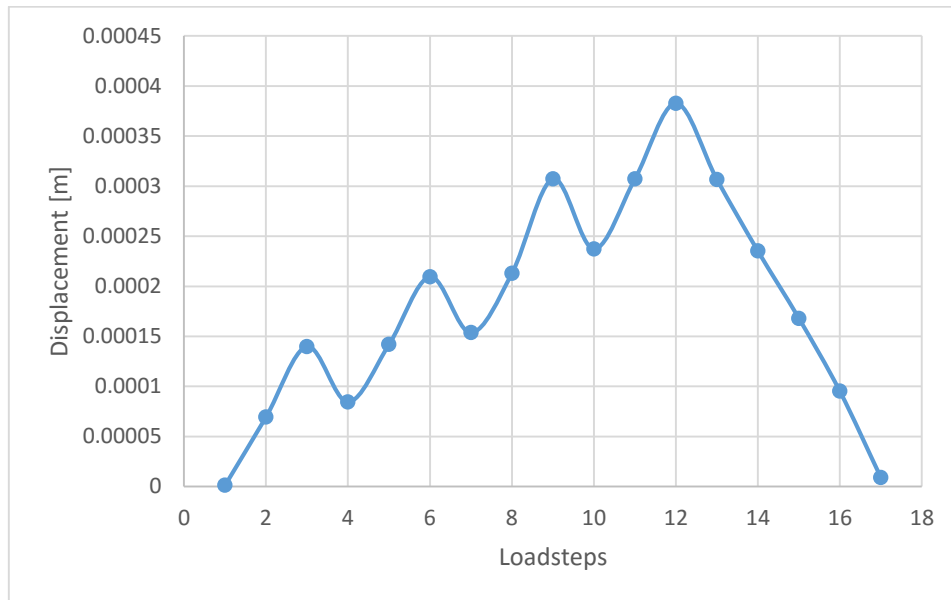


Figure 20 Exemplary displacements of the model

With the parameters for the stresses and strains, a diagram is plotted (Figure 21). Because of the relaxation steps (4, 7 and 10, relieve of strain), a loop is created in the diagram after every relaxation. The Young's Modulus ($E_{RM,3DEC}$) is then calculated with the slope of this loop and the two subsequent loops. The final E_{RM} is the average of those three ($n = 3$).

$$E_{rm,3DEC} = \frac{1}{n} \left(\sum_{i=1}^n \frac{\Delta \sigma_n}{\Delta \epsilon_n} \right) \quad \text{eq. 24}$$

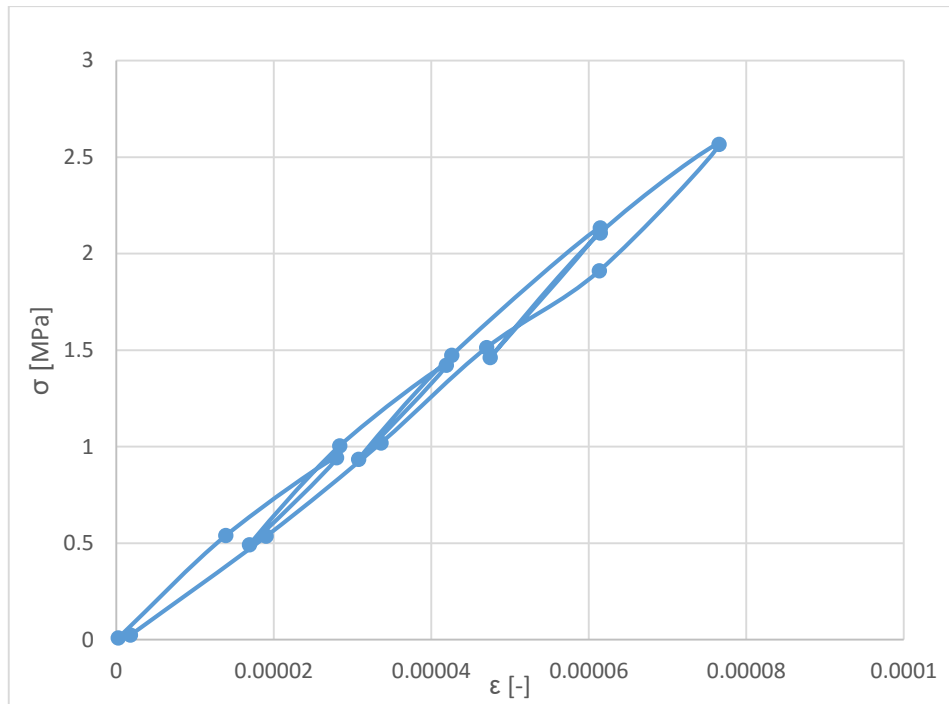


Figure 21 Exemplary stress-strain diagram

5 Results

5.1 Influence of V_b and the block shape

In the following sections, different cases are presented in order to validate the numerical results with the chosen input parameters and empirical solutions. The models are restricted to no (chap. 5.1.1), one (chap. 5.1.2 and 5.1.3) two (chap. 5.1.4 and 5.1.5) and finally three discontinuity sets (chap.5.1.6).

5.1.1 Whole Block

The first model created is a block without any joints, therefore titled “Whole Block”. The purpose of this is to verify that the parameters produced by the model are realistic. As this model has no joints the calculated E_{RM} has to be the same as the pre-set Young’s Modulus. The numerical solution and the “best” case empirical solution have both 50 GPa as a result, therefore in those two cases the E_{RM} is equal to the E_i . For this case no comparison between the three cases was needed.

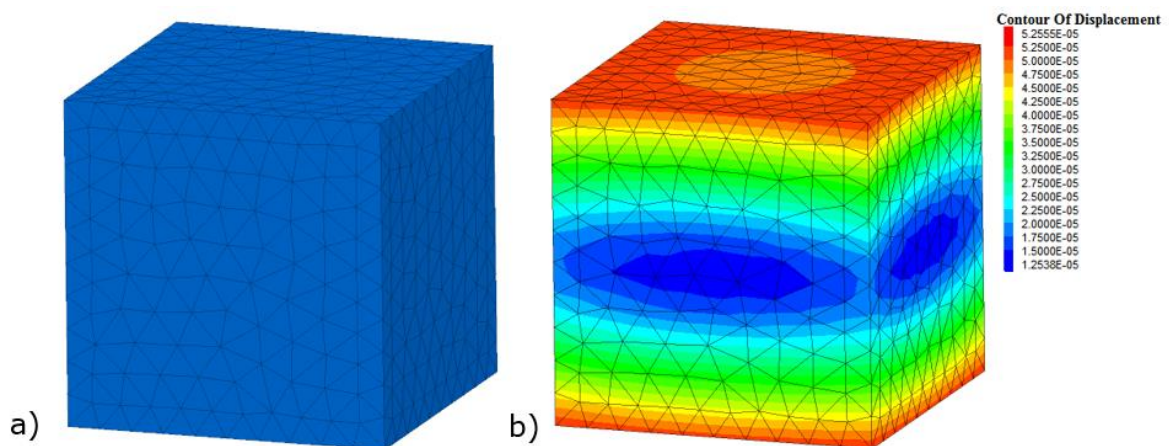


Figure 22 "Whole Block" model a) blocks b)Contour of Displacement

5.1.2 Sandwich

This model is layered horizontally with one joint set which is perpendicular to the z-axis and has a spacing of 1 m; thus its name is “Sandwich” model. For a model with the joint sets defined as such, a different empirical method is available, the “Sandwich Model” (chap. 4.2.2). The E_{RM} calculated with this method, the E_G , is very similar to the result of the numerical analysis, and both are slightly lower than the “best” case when using the block volume GSI evaluation.

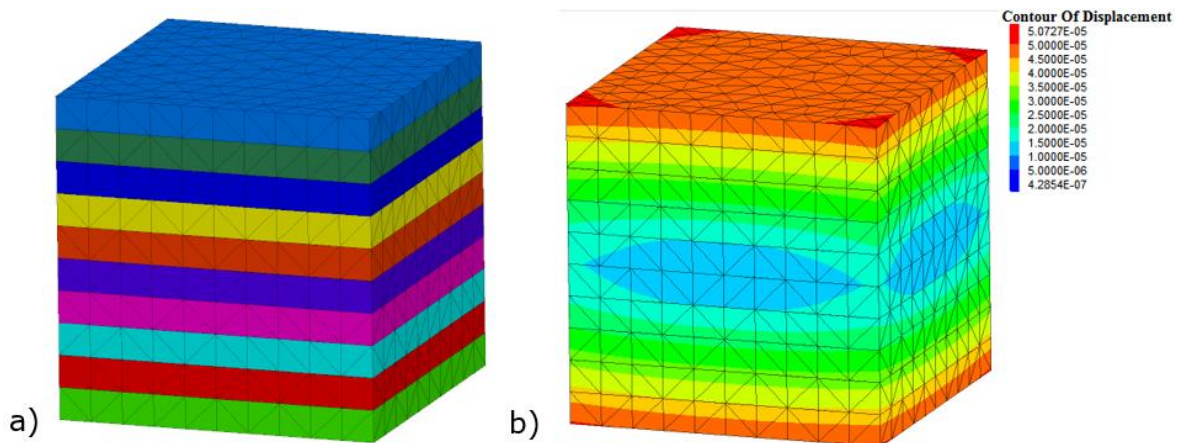


Figure 23 “Sandwich” model a) blocks b) Contour of Displacement

Table 10 Comparison of the resulting rock parameters for “Sandwich”

Case	GSI			3DEC	Sandwich
	best	worst	average	-	-
V_b [cm ³]	1.00E+08	1.00E+08	1.00E+08	1.00E+08	1.00E+08
GSI(V_b, J_c)	88.1	54.7	67.6	-	-
E_{RM}	47.4	20.1	34.3	45.97	45.87

5.1.3 Vertical Sandwich

The next model is also layered and has only one joint set, in this case perpendicular to the x-axis, thus it is called “Vertical Sandwich”. The resulting E_{RM} of the numerical solution is similar to the “Whole Block” model, therefore the $E_{RM,3DEC}$ is the same as E_i . The results of the empirical solution are lower than the numerical one and exactly the same as the results of the layered block with the joint set perpendicular to the z-axis.

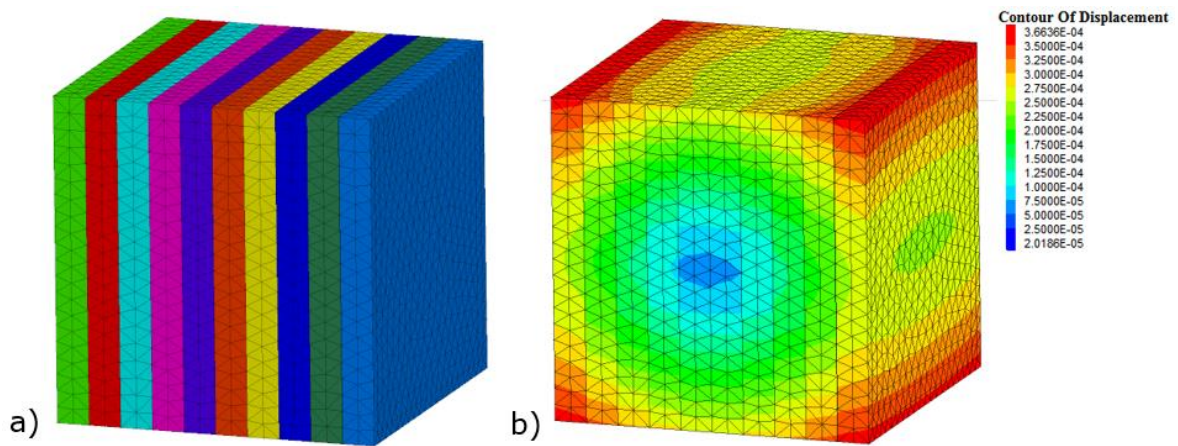


Figure 24 “Vertical Sandwich” model a) blocks b) Contour of Displacement

Table 11 Comparison of the resulting rock parameters for “Vertical Sandwich”

Case	GSI			3DEC
	best	worst	average	-
V_b [cm ³]	1.00E+08	1.00E+08	1.00E+08	1.00E+08
GSI(V_b, J_c)	88.1	54.7	67.6	-
E_{RM}	47.4	20.1	34.3	50.3

5.1.4 Column

This model has two joint sets, both perpendicular to the x-axis and the y-axis, therefore creating columns, hence the “Column” model. The numerical solution for the E_{RM} is very similar to the E_i , while on the other hand the empirical values are considerably lower.

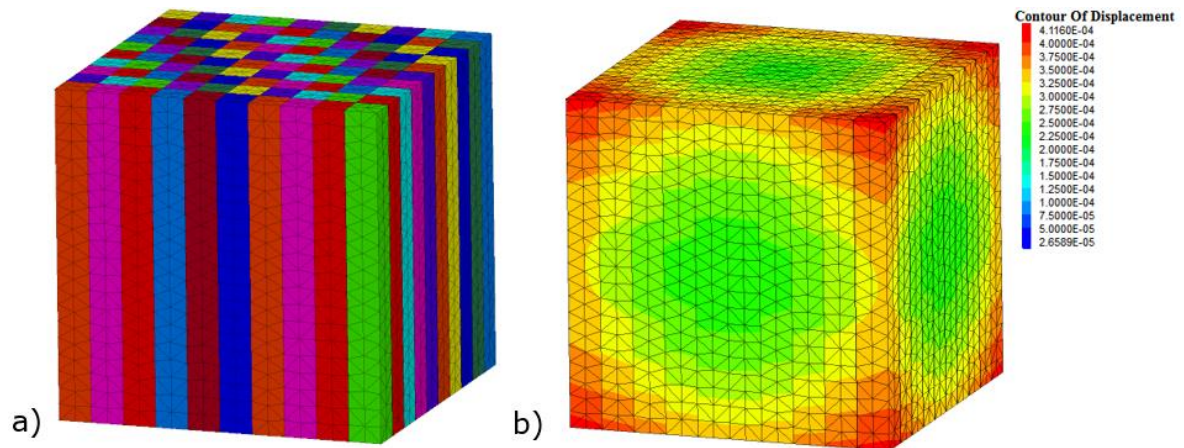


Figure 25 "Column" model a) blocks b) Contour of Displacement

Table 12 Comparison of the resulting rock parameters for “Column”

Case	GSI			3DEC
	best	worst	average	-
V_b [cm ³]	1.00E+07	1.00E+07	1.00E+07	1.00E+07
GSI(V_b, J_c)	76.1	45.4	57.2	-
E_{RM}	41.6	11.5	22.9	50.57

5.1.5 Beam

In this model two joint sets are applied, one perpendicular to the x-axis and one perpendicular to the z-axis. While the empirical solution produces the same as the “Column” model, because the block volume and the joint condition factor are the same, the numerical solution is closer to the result from chapter 5.1.2.

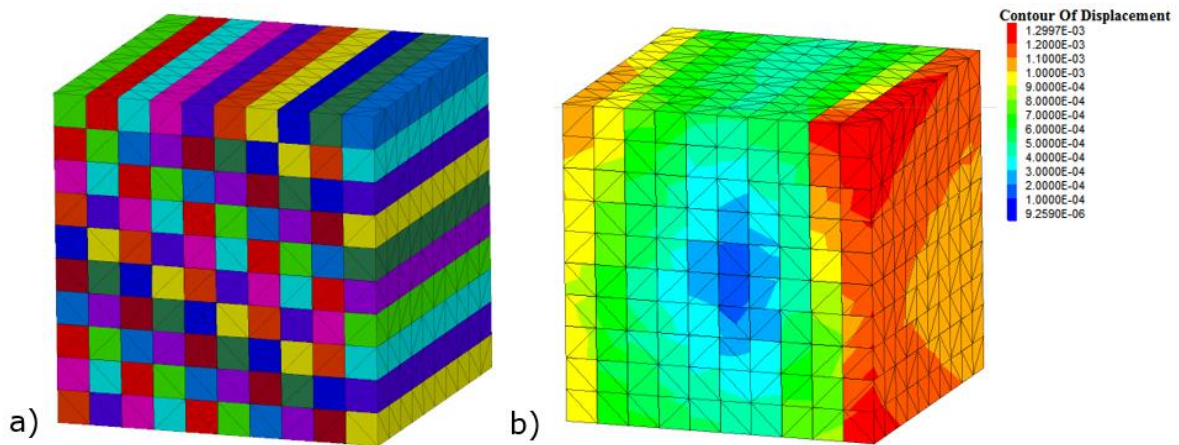


Figure 26 "Beam" model a) blocks b) Contour of Displacement

Table 13 Comparison of the resulting rock parameters for "Beam"

Case	GSI			3DEC
	best	worst	average	-
V_b [cm ³]	1.00E+07	1.00E+07	1.00E+07	1.00E+07
GSI(V_b, J_c)	76.1	45.4	57.2	-
E_{RM}	41.6	11.5	22.9	45.17

5.1.6 Three joint sets (3JS)

In the last validation model, three joint sets are introduced with a joint normal spacing of 1 m. The results show that the difference between the empirical solution for the E_{RM} and the numerical one is increasing.

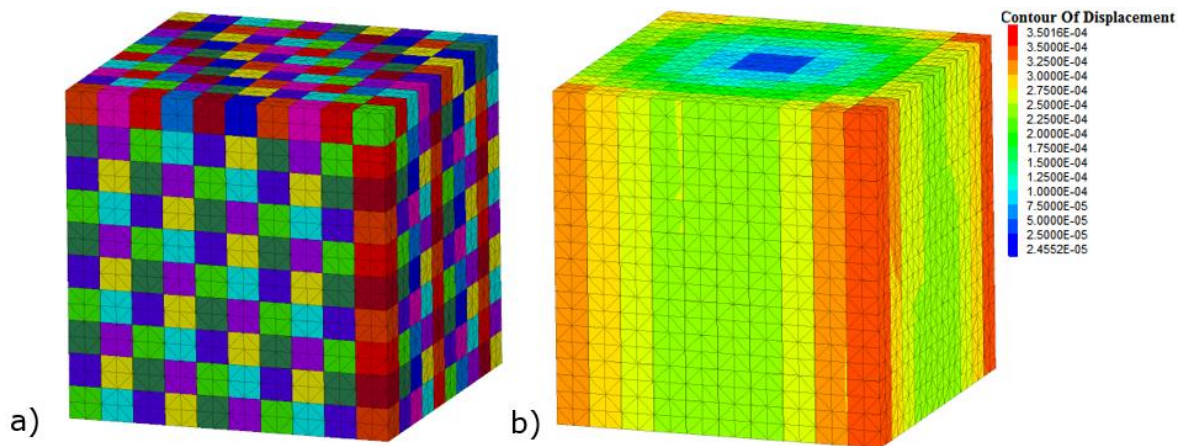


Figure 27 "3JS" model a) blocks b) Contour of Displacement

Table 14 Comparison of the resulting rock parameters for "3JS"

Case	GSI			3DEC
	best	worst	average	-
V_b [cm ³]	1.00E+06	1.00E+06	1.00E+06	1.00E+06
GSI(V_b, J_c)	66.2	37.8	48.7	-
E_{RM}	32.9	6.9	14.2	44.53

To further investigate the impact of V_b , the "3JS" model was taken as basis. From this model the spacing of the joints was varied in order to reduce or increase the resulting V_b . It is important to note that the orientation of the joint sets is still orthogonal to each other. The blocks created from the modified joint sets vary mainly in form and size, from cubic-shaped to plates and from very large volumes to the smallest computable blocks, this is illustrated in Figure 28. For better illustration of the various results, especially in the case of smaller block volumes, a logarithmic scale is used in Figure 29.

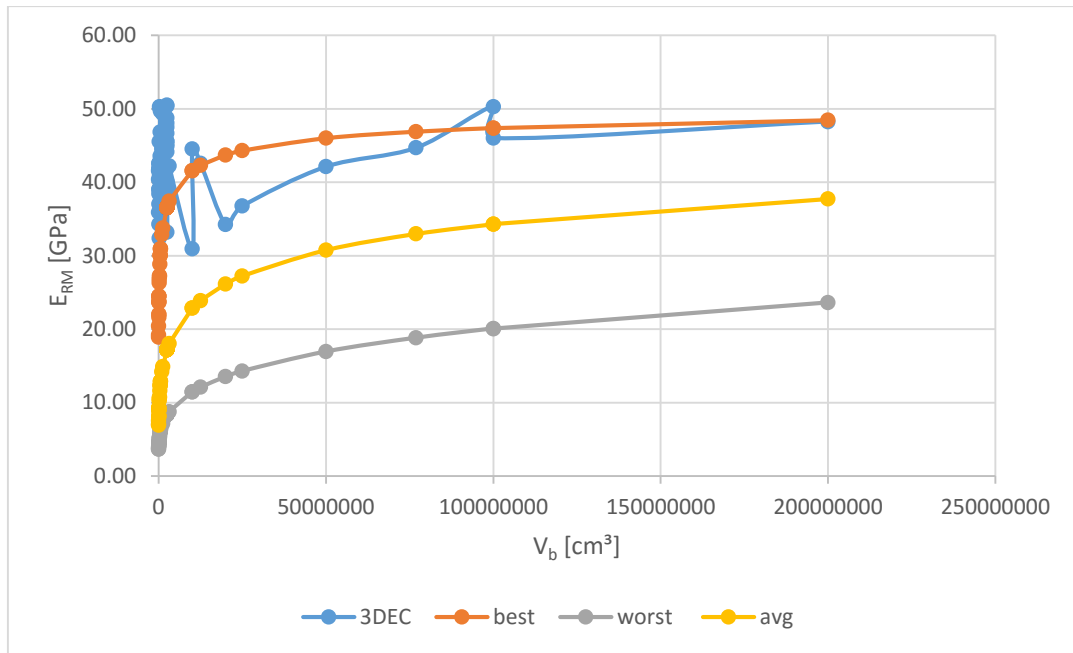


Figure 28 Block Volume and correlation of the E_{RM}

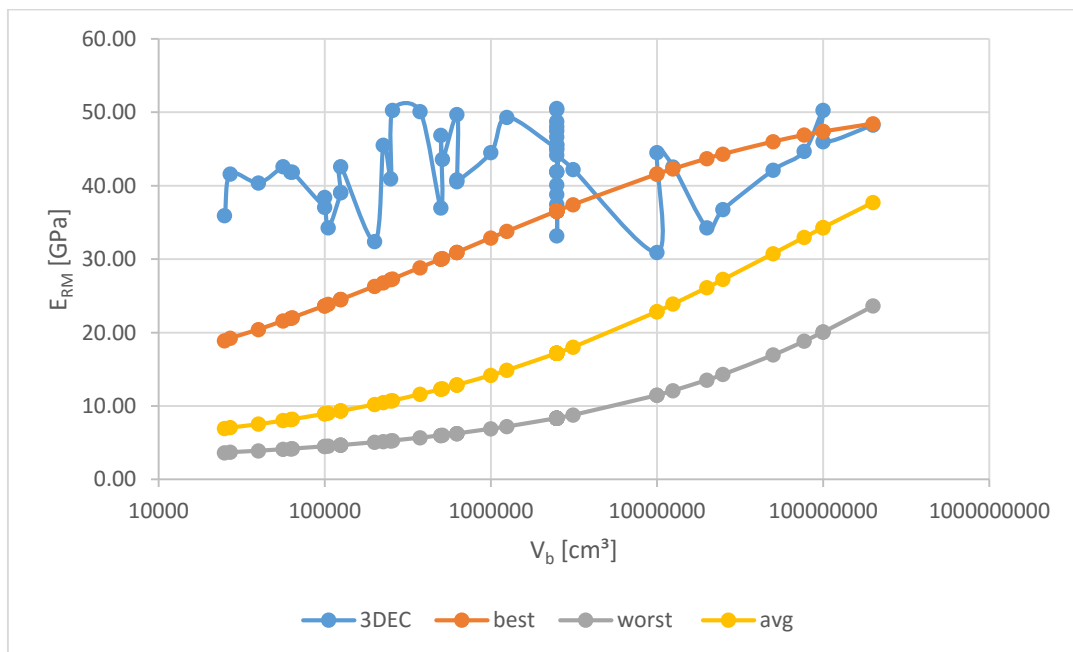


Figure 29 Block Volume and correlation of the E_{RM} in logarithmic scale

5.2 Influence of the persistence

The persistence describes the continuity of joints and can rank from 0.0 to 1.0. Naturally with lower persistence, block volumes will be larger. This can be seen easily when comparing Figure 30, where a model with a persistence of a) 0.3 and b) 0.8 is pictured. According to the aim of this thesis, the persistence of all three joint sets was varied to investigate the sensitivity of the model on the persistence. The sensitivity analysis was applied on an orthogonal joint network with three joint sets.

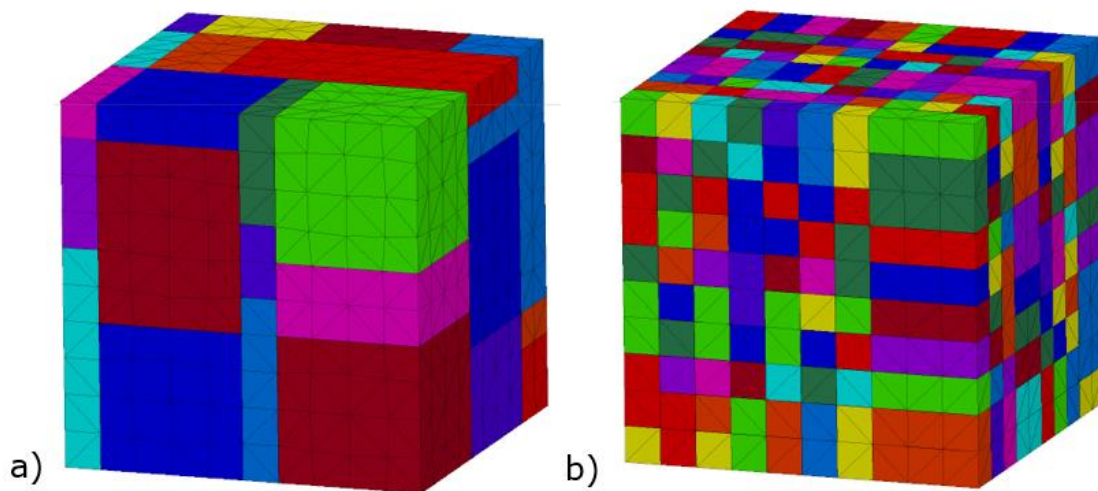


Figure 30 Block with a persistence of a) 0.3 and b) 0.8

The impact of the persistence on the V_b is illustrated in Figure 31 with the axis for V_b in logarithmic scale.

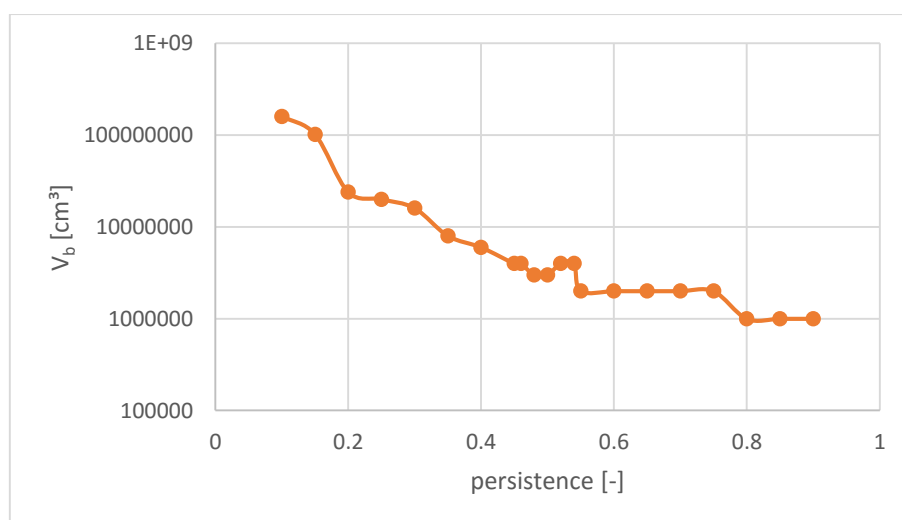


Figure 31 V_b according to the persistence of the joint sets in logarithmic scale

The impact of the persistence on the $E_{RM,3DEC}$ is illustrated in Figure 32.

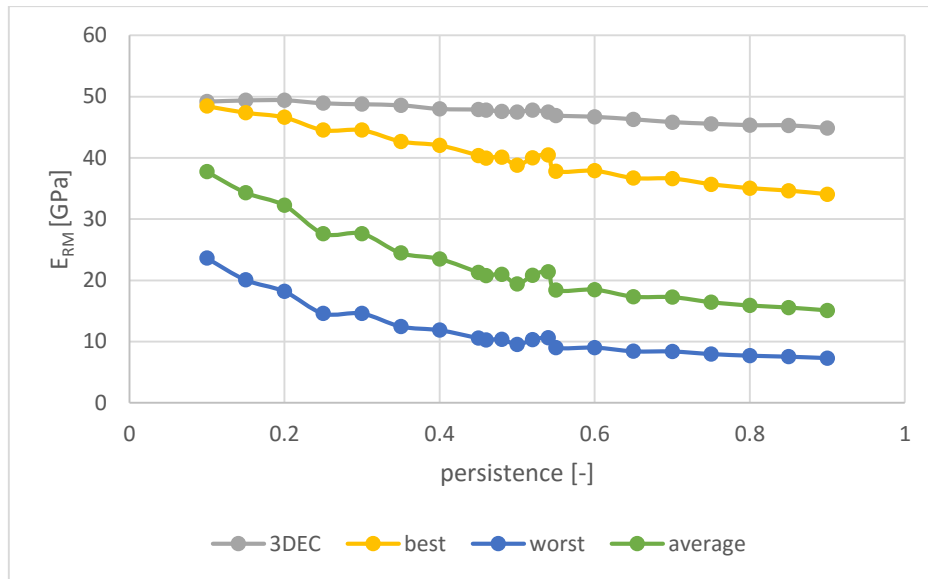


Figure 32 E_{RM} in relation to the persistence

5.3 Influence of other parameters

The following parameters have no impact on the empirical values, as they don't include any of them, therefore only their impact on the $E_{RM,3DEC}$ is described in this chapter.

5.3.1 Joint normal stiffness

The joint normal stiffness (jkn) for the joints of the models was predefined to be 500 GPa. This value was chosen according to a sensitivity analysis with a series of models with a different value for the jkn . The results are plotted in Figure 33. The chosen values range from 300 to 800 GPa. The $E_{RM,3dec}$ for a "3JS" model ranges between 42 GPa and 46 GPa Figure 33. .

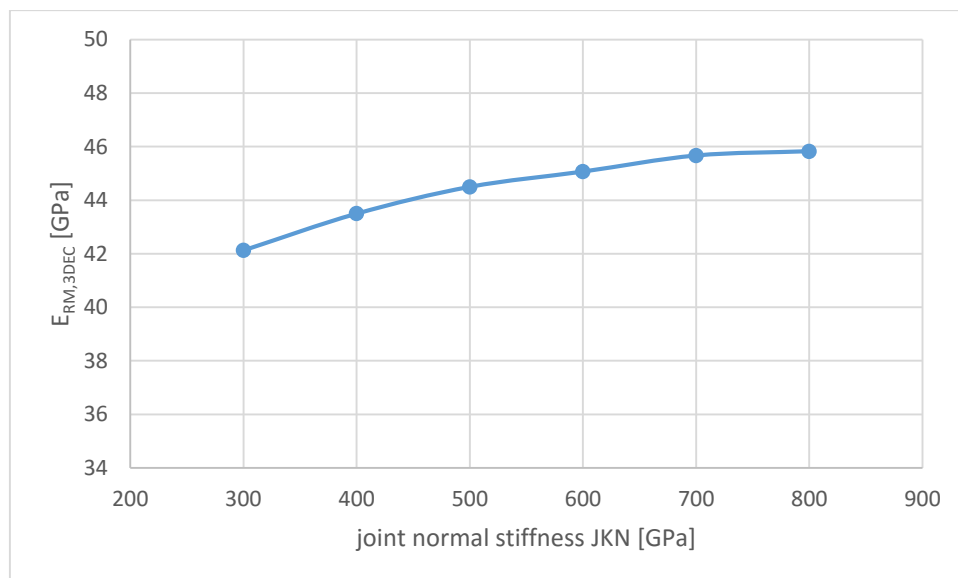


Figure 33 Impact of the joint normal stiffness jkn on the $E_{RM,3DEC}$

To verify the model also unrealistic joint normal stiffness were tested, for example 5,000 GPa which lead to an extremely high $E_{RM,3DEC}$. Additionally, a low jkn of 50 GPa, was tested, resulting in a very low $E_{RM,3DEC}$ of 26 GPa.

5.3.2 Influence of inclined of joints

When investigating the impact of the joint set inclination, it became clear that a shear failure is occurring (Figure 34). To prevent shearing in future analyses it is recommended to simulate a triaxial compression test to investigate the impact of the joint orientation.

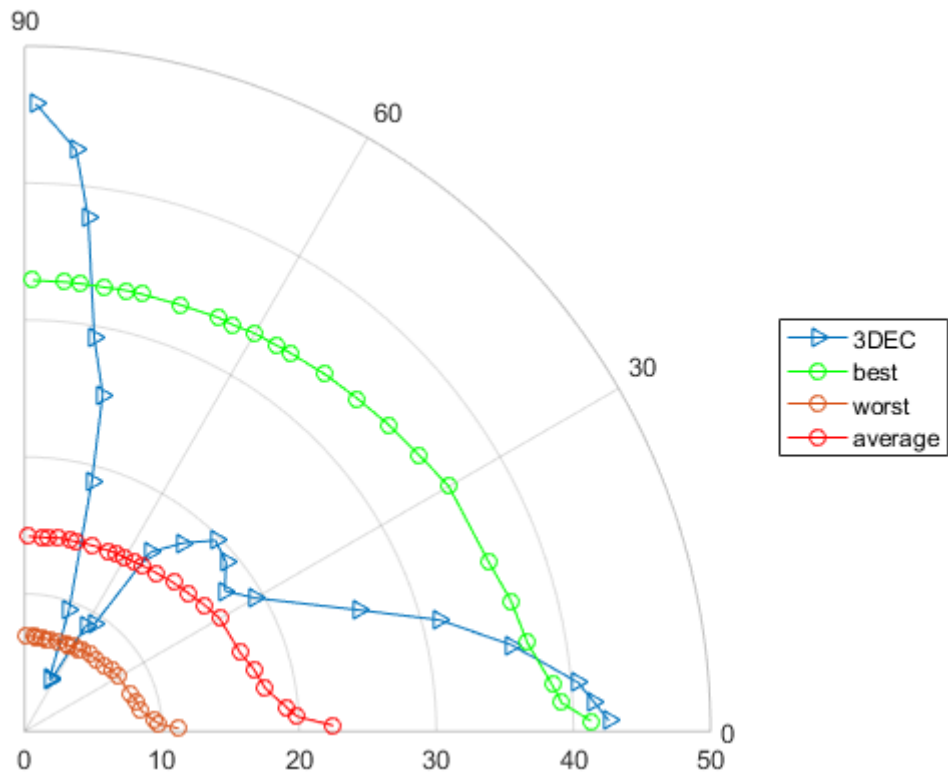


Figure 34 Dip angle polar diagram

6 Interpretation and Discussion

6.1 Influence of V_b

Analysing the results, one can see that the influence of the block size on the stiffness of the rock mass to a great extent is influenced by the loading direction in relation to the joint orientation. As an example the column model shall serve: adding additional joints parallel to the loading direction decreases the block volume, practically no influence on the E-modulus can be observed. On the other hand, when using the empirical relationship of Cai et al [14], the block volume has a significant influence on the rock mass stiffness.

It can be clearly seen that the empirical relationships just refer to two-dimensional problems, and even here do not consider the influence of different loading directions in relation to the discontinuity orientation.

6.1.1 Block shapes

To show the influence of the block shape, the different models are plotted separately according to the shape classes, defined in chapter 4.1.2.1. To better present the various models the plots are all with logarithmic scale for V_b . Since some shapes have a large range of possible combinations of the spacing it is possible that some models have the same block volume, but a different E_{RM} , because the dimensions are slightly different. All calculations are based on an orthogonal joint network.

6.1.1.1 Cubic shaped

Cubic blocks are generated with an equal joint normal spacing for all three discontinuity sets and intersection angles of 90° . $E_{RM,3DEC}$ only decreases slightly, even at very small values for the spacing and the resulting block volume. The significant impact of the reduced V_b on $E_{RM,GSI}$ and its minor influence on $E_{RM,3DEC}$ is quite obvious (Figure 35).

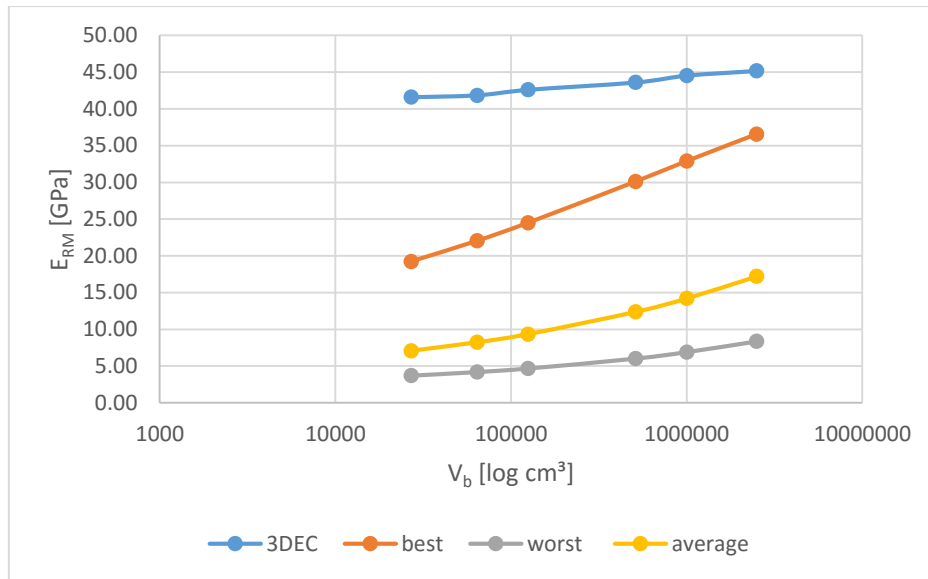


Figure 35 Comparison of the $E_{RM,3DEC}$ [GPa] with the $E_{RM,GSI}$ [GPa] for cubes

6.1.1.2 Columnar shaped

In general, the $E_{RM,3DEC}$ is very high and almost equals E_i in columnar shaped blocks. (Figure 36). The columnar shaped blocks show the highest values for the Young’s modulus of the modelled rock mass. The independence of $E_{RM,3DEC}$ from V_b is even more obvious than for cubic shaped blocks. In some cases, the 3DEC produces results with the Young’s moduli even exceeding E_i . In the following this is referred to as “plate problem” (chap.6.1.1). Obvious case with unrealistic results are excluded from Figure 36.

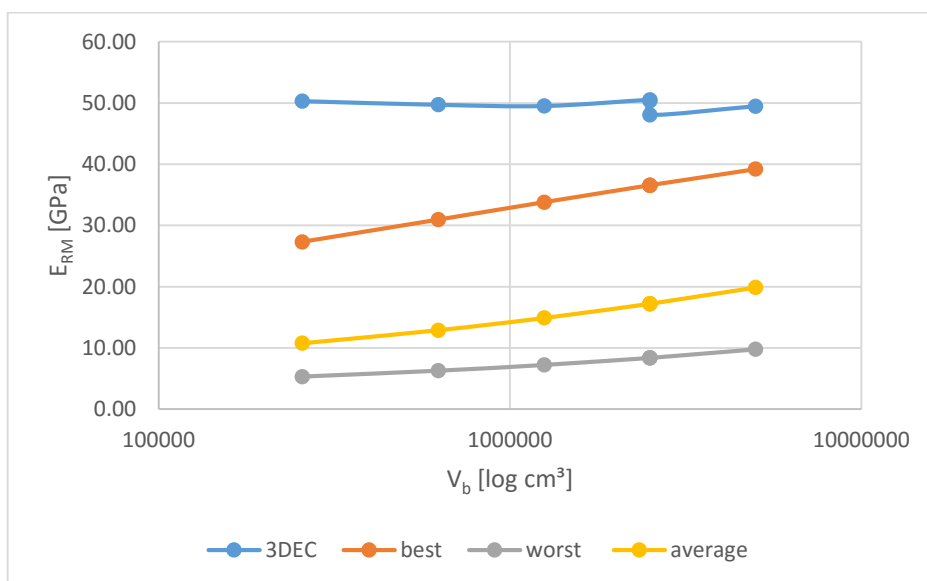


Figure 36 Comparison of the $E_{RM,3DEC}$ [GPa] with the $E_{RM,GSI}$ [GPa] for columns

6.1.1.3 Plate shaped

The $E_{RM,3DEC}$ of the plate shaped blocks tend to be higher than the average E_{RM} for a “3JS” model which is around 45 GPa, in some cases almost like E_i , and is therefore comparable to the column models. Again, the models with the “plate problem” (chapter 6.1.1) are excluded from the data of Figure 37.

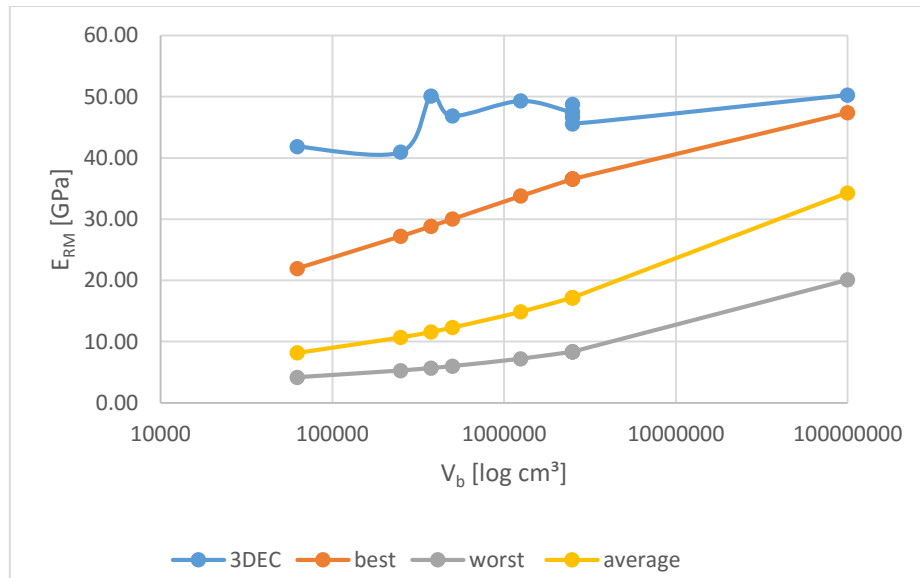


Figure 37 Comparison of the $E_{RM,3DEC}$ [GPa] with the $E_{RM,GSI}$ [GPa] for plates

6.1.1.4 Beam shaped

The results of $E_{RM,3DEC}$ for the beam shaped blocks are usually higher than the best case, but do not tend to be higher than the “3JS”-model from chapter 5.1.6, as can be seen in Figure 38 .

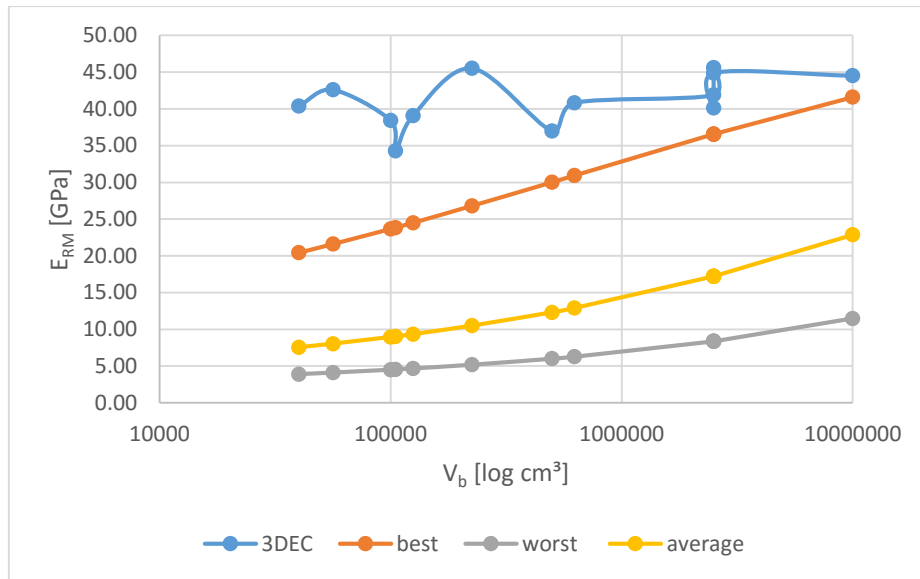


Figure 38 Comparison of the $E_{RM,3DEC}$ [GPa] with the $E_{RM,GSI}$ [GPa] for beams

6.1.1.5 Slab shaped

The slab shaped models are quite interesting as they are the only ones that are in some cases lower than the anticipated best case of $E_{RM,GSI}$ (Figure 36). They are generally below average and can be considered the shape that generates the lowest E_{RM} with similar V_b .

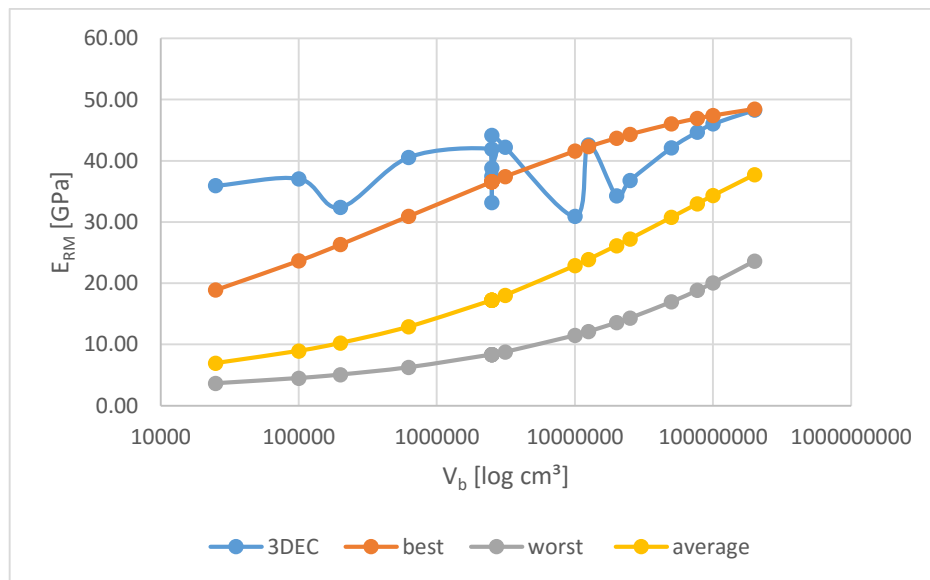


Figure 39 Comparison of the $E_{RM,3DEC}$ [GPa] with the $E_{RM,GSI}$ [GPa] for slabs

6.1.2 Influence of the block shape

It is difficult to directly compare the resulting E_{RM} for the different block shapes, because of the range of possible V_b that each shape class create. Therefore 17 models with a constant V_b of $2.5 \cdot 10^6 \text{ cm}^3$ are compared to show the influence of the block shape on the $E_{RM,3DEC}$. In Figure 40 a box whisker plot of the different shape classes is illustrated. The cube shape is illustrated as a line because only one cubic model is possible for a predefined V_b .

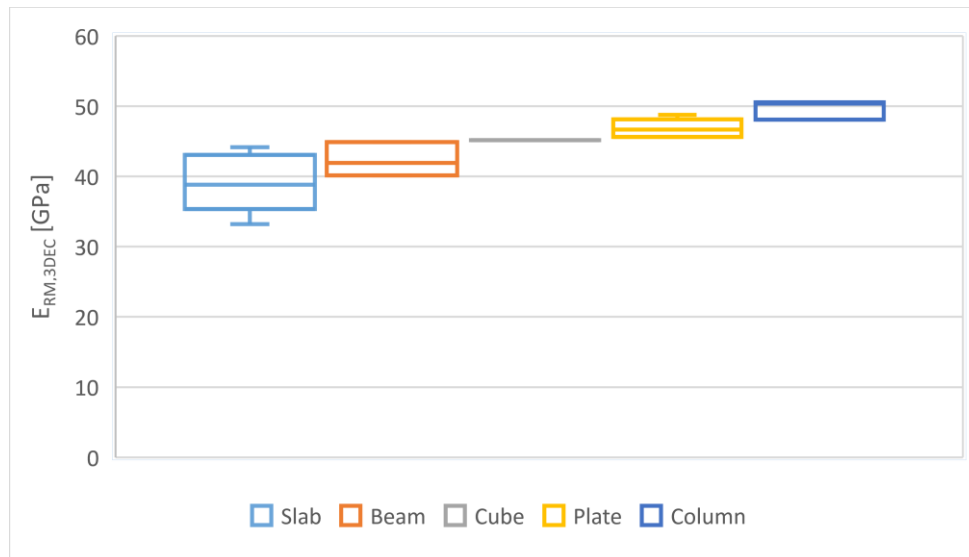


Figure 40 $E_{RM,3DEC}$ for $V_b 2,5 \cdot 10^6 \text{ [cm}^3\text{]}$ by shape in a box whisker plot

The diagram indicates that the slab and beam shaped blocks generally express a lower $E_{RM,3DEC}$ than the plate and column shaped blocks.

This leads to the conclusion, that shapes with a with a closely spaced joint perpendicular to the load direction generally show a lower E_{RM} than in models with a joint set striking parallel to the load orientation.

6.1.3 Impact of the joint spacing

It is obvious that the $E_{RM,3DEC}$ for slab and beam shaped blocks is generally lower, therefore one can assume that the spacing perpendicular to the loading has major impact on the results. To show the impact of the spacing perpendicular to the loading, models with the same block volume are compared. The block volume chosen for this was $2,5 \cdot 10^6 \text{ cm}^3$. This block volume allowed many possible combinations for the spacing, and therefore covering all possible block shape classes.

The results are listed in Table 15 and illustrated in Figure 41. The empirical values are added to the graph to show that with a constant volume, the $E_{RM,GSI}$ stays constant as well. It is quite obvious that a closely spaced joint perpendicular to the load direction the smallest E_{RM} generates. Once this spacing is kept constant, the shape significant parameter for the $E_{RM,3DEC}$ is the block shape.

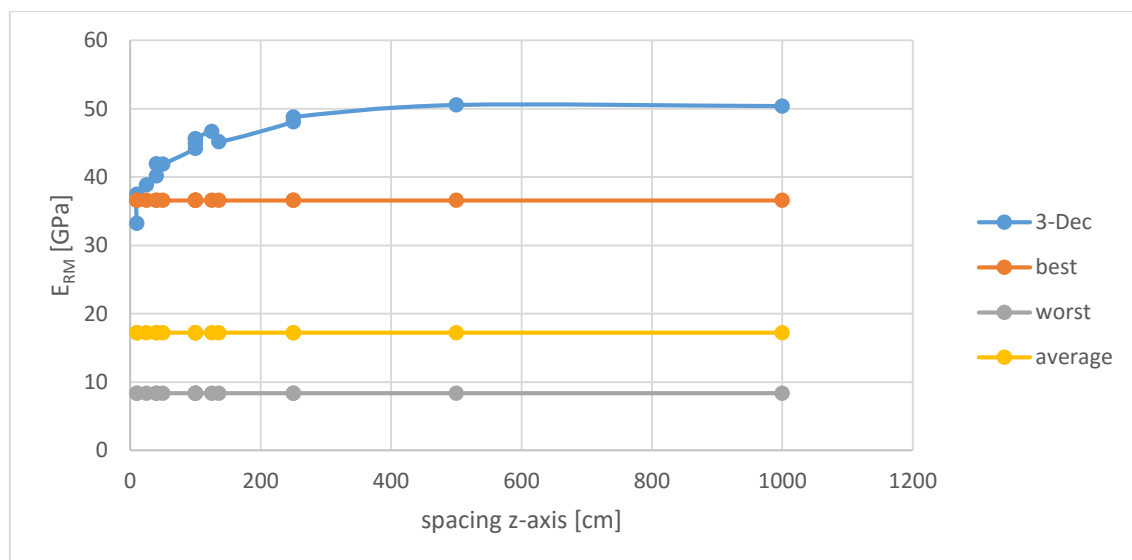


Figure 41 E_{RM} for $V_b 2,5 \cdot 10^6 \text{ [cm}^3\text{]}$

The shape classes are listed in the following according to the ascending potential to generate high $E_{RM,3DEC}$:

1. Slab shape
2. Beam shape
3. Cube shape
4. Plate shape
5. Column shape

Models where the “plate problem” occurs are excluded in the chart.

Table 15 $E_{RM,3DEC}$ for $V_b = 2,5 \cdot 10^6$ [cm³]

$E_{RM,3DEC}$	sp1[cm]	sp2[cm]	sp3[cm]	Shape
33.2	500	500	10	Slab
37.47	250	1000	10	Slab
38.83	500	200	25	Slab
40.13	125	500	40	Beam
41.93	250	250	40	Slab
41.9	1000	50	50	Beam
44.5	125	200	100	Slab
44.9	250	100	100	Beam
45.6	50	500	100	Plate
46.67	40	500	125	Plate
48.07	100	100	250	Column
48.77	40	250	250	Plate
50.53	40	125	500	Column
50.37	50	50	1000	Column

6.1.4 “Plate Problem”

During the evaluation of the results, the so called “plate problem” occurred. This problem refers to several exceptions, where $E_{RM,3DEC}$ was higher than E_i , which obviously is not possible, since the Young’s Modulus of a jointed rock mass cannot be higher than that of an intact rock. The “plate problem” occurs when a joint set, striking parallel to the loading direction is narrowly spaced (0.1 m to 0.15 m), and the second spacing of a joint set striking parallel to the loading direction is considerably wider (0.5 m to 10 m).

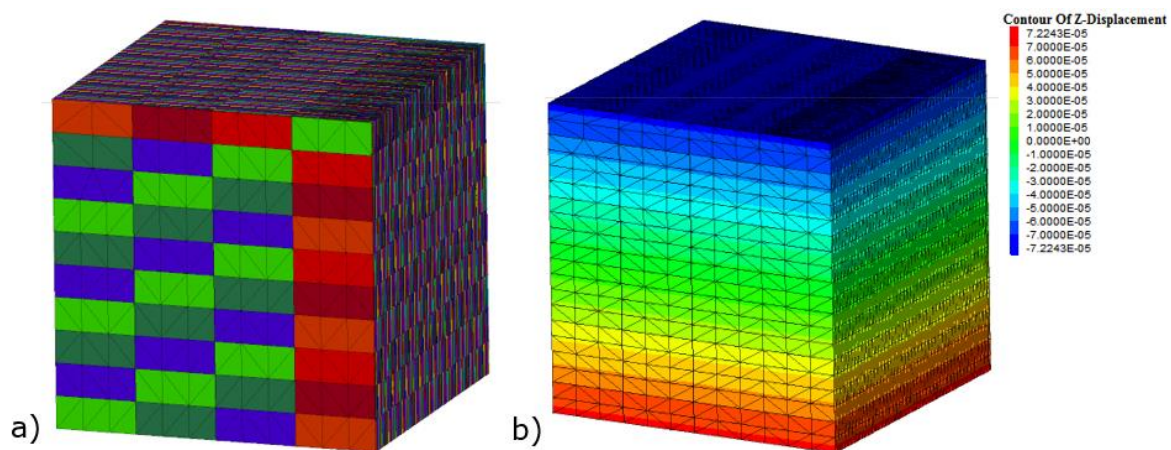


Figure 42 Exemplary a) model and b) contour of the z-displacement for the “plate problem”

The height of the block has to be at least 0.5 m. This configuration generates a plate, comparable to the “Vertical Sandwich” model. Due to the definition of shapes some of those models are by definition columns, even though they could be considered to be a plates and fit into the boundary conditions for this problem.

The models with this problem as well as the values for the joint spacing are listed in Table 16. The table shows that the most decisive parameter is the spacing for the sp1 or x. When x equals 15 cm, $E_{RM,3DEC}$ is already considerably higher than the E_i , when this spacing is reduced even further (10 cm), E_{RM} is more than 25 % higher than the E_i .

The reason for this problem is yet not fully understood and needs further investigations. However, it only appears in cases with a special set of boundary conditions. It is possible to conclude that models not subject to such a boundary condition can still be considered providing realistic results.

Table 16 List of E_{RM} [GPa] for "Plate" Problems with the corresponding spacing of the joint sets in [cm]

$E_{RM,3DEC}$	sp1 [cm]	sp2[cm]	sp3[cm]
52.67	15	500	500
53.47	15	1000	1000
54.7	10	1000	1000
54.97	15	250	250
57.77	10	100	1000
61.3	10	250	100
62.37	10	250	50
62.77	10	500	50
63.2	10	1000	50
64.4	10	100	100

6.2 Influence of the persistence

The influence of the persistence is analysed on the basis of the “3JS” model. The persistence can only increase the possible E_{RM} , therefore it can only be between the E_{RM} of the “3JS” model and the “Whole Block” model. This two models represent the boundaries of the analysis, because the “3JS” model has a persistence of 1.0 and the “Whole Block” represents a model with the persistence of 0.0.

The impact of the persistence on the V_b is illustrated in Figure 31 with the axis for the block volume in logarithmic scale. It should be noted that when the persistence ranges between 0.45 to 0.55, the results are varying in such a degree, that a direct correlation is not recognisable. The reason for this is presumably the fact that the splitting of the blocks is happening in accordance to a probability, hence it is possible that the median average of the V_b of the model that is split at a probability of 0.48 is very similar to the one split with a persistence of 0.52.

In Figure 32 $E_{RM,GSI}$ is compared with the $E_{RM,3DEC}$ in regard of the persistence and again, the disconnection of V_b with $E_{RM,3DEC}$ is apparent. In the empirical solution there is no steady increase of $E_{RM,GSI}$ between the values 0.45 and 0.55, this is due to the irregular correlation between the V_b and the persistence in this range. In contrast, $E_{RM,3DEC}$ increases steadily with the decrease of the persistence.

Because the persistence creates a number of very different blocks for each new model it is not possible to directly show the impact of the spacing and the block shape on the E_{RM} . Therefore, a “reference spacing” or s_{pref} had to be used. This s_{pref} is based on the median V_b and its cube root. This is a vast simplification, but still a clear trend can be identified. The $E_{RM,3DEC}$ is not reduced constantly, with a decreasing s_{pref} , as shown in Figure 43. This is due to the fact that the blocks are split by probability. In Table 17 the persistence is listed with the $E_{RM,3DEC}$ and the s_{pref} . It can be seen that the inconstancy occurs again in the range from 0.45 to 0.55. In Figure 43 the trend line is plotted as a dotted line. This trend line shows that there is still a clear trend of the E_{RM} , decreasing with s_{pref} .

One has to be careful not to conclude that the persistence is an evidence for a correlation between the block volume and $E_{RM,3DEC}$. Generally spoken a lower persistence means an increase in the probability of larger blocks, which increase the probability of having a large number of blocks with an increased spacing perpendicular to the load. This on the other hand leads to an increase in the E_{RM} .

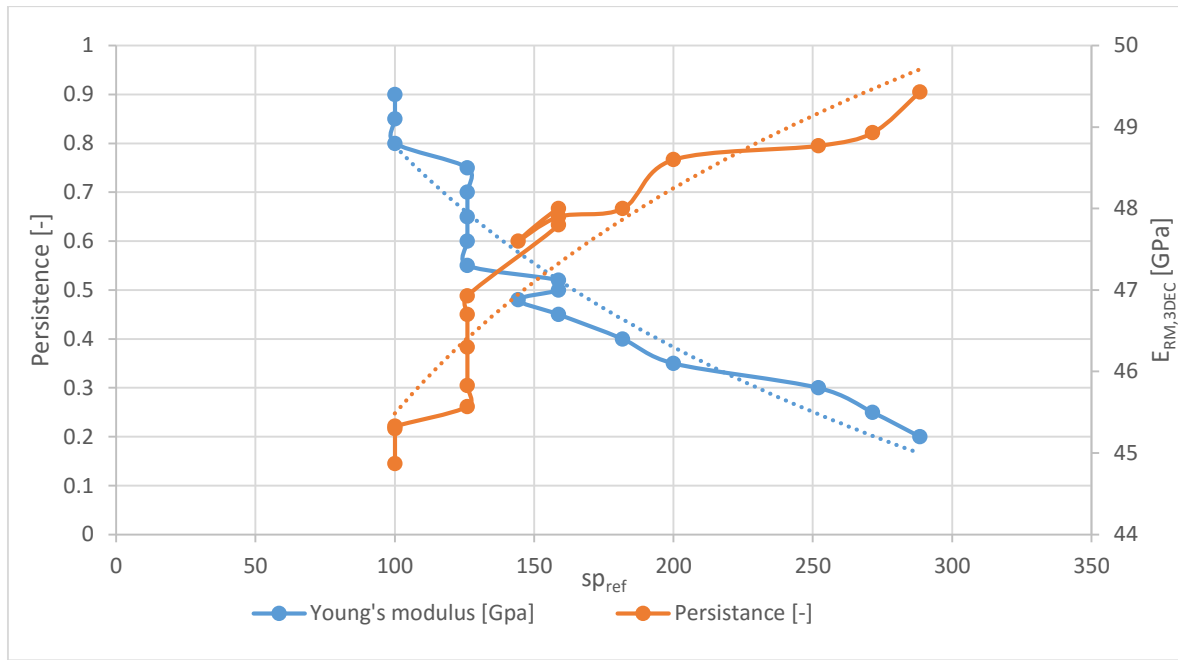


Figure 43 $E_{RM,3DEC}$ for the "median average spacing", the dashed lines indicate the fitted trend lines

Table 17 List of the persistence with correlating $E_{RM,3DEC}$ and the reference spacing (sp_{ref})

Persistence [-]	$E_{RM,3DEC}$ [GPa]	sp_{ref} [cm]
0.2	49.43	288
0.25	48.93	271
0.3	48.77	252
0.35	48.6	200
0.4	48	182
0.45	47.9	159
0.48	47.6	144
0.5	48	159
0.52	47.8	159
0.55	46.93	126
0.6	46.7	126
0.65	46.3	126
0.7	45.83	126
0.75	45.57	126
0.8	45.33	100
0.85	45.3	100
0.9	44.87	100

7 Conclusion and Outlook

With the investigations conducted in the course of this thesis it could be shown that current empirical rock mass characterization methods are oversimplified and may lead to misleading results. The main deficiency of those methods is that they do not consider the spatial discontinuity distribution, but are extrapolating two-dimensional evaluations into the volume. This may not significantly influence the results in case the degree of fracturing is approximately similar in all directions, but has a big influence in case of anisotropic rock masses with arbitrary block shapes and joint set spacing.

The case studies showed that the rock mass stiffness prominently is influenced by the relative orientation between load orientation and dominant joint orientations, respectively the block shape.

Future works in this field might include simulations with a three-dimensional stress field, enabling also to model non-perpendicular joint sets.

The reasons for unrealistic results of the numerical model for certain joint set configurations requires clarification as well.

8 References

- [1] Hoek E, Marinos P, Benissi M. Applicability of the geological strength index (GSI) classification for very weak and sheared rock masses. The case of the Athens Schist Formation. *Bull Eng Geol Environ* 1998;57(2):151–60.
- [2] Cai M, Kaiser PK, Uno H, Tasaka Y, Minami M. Estimation of rock mass deformation modulus and strength of jointed hard rock masses using the GSI system. *International Journal of Rock Mechanics and Mining Sciences* 2004;41(1):3–19.
- [3] Hoek E, Brown E. Empirical strength criterion for rock masses. *Journal of Geotechnical and Geoenvironmental Engineering* 1980:1013–5.
- [4] Bieniawski ZT. *Engineering rock mass classifications: A complete manual for engineers and geologists in mining, civil and petroleum engineering / Z. T. Bieniawski.* New York, N.Y.: Wiley; 1989.
- [5] Hoek E, Carranza-Torres C, Corkum Brent (eds.). *Hoek-Brown failure criterion - 2002 Edition*; 2002.
- [6] Marinos P, Hoek E. GSI: A geologically friendly tool for rock mass strength estimation 2000:1–19.
- [7] Hoek E, Marinos P. A brief history of the development of the Hoek-Brown failure criterion. *Soils and Rocks* 2007.
- [8] Hustrulid WA, McCarter MK, van Zyl DJA. *Slope stability in surface mining: Slope Stability at Aznalcóllar.* Littleton, CO: Society for Mining; 2000.
- [9] Sonmez H, Ulusay R. Modifications to the geological strength index (GSI) and their applicability to stability of slopes. *International Journal of Rock Mechanics and Mining Sciences* 1999;36(6):743–60.
- [10] Hoek E. Blast Damage Factor D. Technical note for RocNews - February 2, 2012 2012.
- [11] Barton N. Barton, Lien and Lunde, 1974. Engineering classification of rock masses for.
- [12] Hoek E, Marinos PG, Marinos VP. Characterisation and engineering properties of tectonically undisturbed but lithologically varied sedimentary rock masses. *International Journal of Rock Mechanics and Mining Sciences* 2005;42(2):277–85.
- [13] Marinos P, Hoek E. Estimating the geotechnical properties of heterogeneous rock masses such as flysch. *Bulletin of Engineering Geology and the Environment* 2001;60(2):85–92.
- [14] Cai M, Kaiser PK, Tasaka Y, Minami M. Determination of residual strength parameters of jointed rock masses using the GSI system. *International Journal of Rock*

- Mechanics and Mining Sciences 2007;44(2):247–65.
- [15] Kim BH, Cai M, Kaiser PK, Yang HS. Estimation of Block Sizes for Rock Masses with Non-persistent Joints. *Rock Mech. Rock Engng.* 2007;40(2):169–92.
- [16] Cai M, Kaiser P. Visualization of rock mass classification systems. *Geotech Geol Eng* 2006;24(4):1089–102.
- [17] Hoek E, Carter TG, Diederichs MS (eds.). Quantification of the Geological Strength Index chart: American Rock Mechanic Association; 2013.
- [18] Bieniawski ZT. Determining rock mass deformability - experience from case histories. *Int. J. Rdck Mech. Min. Sci. & Geomech, Abstr.* 1978;15:237–47.
- [19] Serafim JL, Pereira JP (eds.). Consideration of the geomechanical classification of Bieniawski; 1983.
- [20] Cai M. Rock Mass Characterization and Rock Property Variability Considerations for Tunnel and Cavern Design. *Rock Mech Rock Eng* 2011;44(4):379–99.
- [21] Hoek E, Diederichs MS. Empirical estimation of rock mass modulus. *International Journal of Rock Mechanics and Mining Sciences* 2006;43(2):203–15.
- [22] Palmström A, Singh R. The deformation modulus of rock masses — comparisons between in situ tests and indirect estimates. *Tunnelling and Underground Space Technology* 2001;16(2):115–31.
- [23] Kalenchuk KS, Diederichs MS, McKinnon S. Characterizing block geometry in jointed rockmasses. *International Journal of Rock Mechanics and Mining Sciences* 2006;43(8):1212–25.
- [24] Schubert W. *Felsmechanik Skriptum*. Graz.
- [25] BSc Kluckner Alexander. *Aspekte der Gebirgscharakterisierung im Tunnelbau* 2012.

9 Internet bibliography

Itasca Consulting Group, Inc. Itasca Homepage. *http://www.itascacg.com/software/3dec*.
[Online] [Cited: 14 8 2017.] *http://www.itascacg.com/software/3dec*.

10 Appendix A

Main File

```
new ;!!!!!!
;-----
;-----Header-----
;-----

set cust1 'Name Surname'
set cust2 'Graz University of Technology'

def sys
    md = 'C:\\...\\...\\' ; Folder location
end
@sys
set directory @md

;-----
;-----Units-----
;-----

;length = [m]
;stress = [MPa]
;force = [MN]

;-----
;--ModelParameter--
;-----

;--Model Boundaries-- [m]
def geometry ;definition for the Model geometry
x1 = 0
x = 10
x2 = x1 + x
y1 = x1
y2 = x2
z1 = x1
```

```
z2 = x2

base = x2*0.05 ;thickness
top = x2*0.05

;---Loading Parameters---
cy = 1000 ;Number of cycles each step runs
pp = 0.1 ; for increasing or decreasing the Load by a factor
edge = 1 ;For the meshing of the model
steps = 17 ;Number of steps for the Load
name = "name" ;Name for the particular model

;-----Side Calcs-----
x3 = x1 - base
x4 = x2 + top

y3 = y1 - base
y4 = y2 + top

z3 = z1 - base
z4 = z2 + top

z5 = z2*(1-1e-3) ; Region where the displacements are applied
z6 = z2*(1+1e-3)
z7 = z2*(-1e-3)
z8 = z2*(1e-3)

;-----Dip-----[°] ;Inclination for the shear planes
dip1 = 90
dip2 = 90
dip3 = 0

;----Dip Direction----[°]
dd1 = 0
dd2 = 90
dd3 = 0

;----Joint Spacing---- [m] ;Spacing between each shear plane
sp1 = 1
sp2 = 1
sp3 = 1

;---Number of Joints---[-]
```



```
num1 = 20
num2 = 20
num3 = 20

;-----Persistence-----[-]
per1 = 1
per2 = 1
per3 = 1

end
@geometry

def inputMaterial

;----Joint Properties----
conj = 2 ; constitutive model (2=Mohr.Coulomb failure)
jkn = 5e5 ; joint normal stiffness [MPa]
jks = 5e3 ; joint shear stiffness [MPa]
phi = 27 ; joint friction angle [°]
coh = 15 ; cohesion [MPa]

;--Material Properties--
conn = 2 ; constitutive model (2=Mohr.Coulomb failure)
rho = 2700*1e-6 ; density [kg/m³]
pratio = 0.25 ; Poisson's ratio [-]
you = 5e4 ; Youngs' modulus [MPa]
bc = 15 ; Block Cohesion [MPa]
bdi = 0 ; dilatation angle [°]
bfri = 30 ; friction angle [°]
btension = 0.7 ; tensile strength [MPa]

bulk = you/(3*(1-2*pratio)) ; block bulk modulus
shear = you/(2*(1+pratio)) ; shear modulus

;--LOAD--- [MN]
Load1= -0.00144;
Load2 = -0.07603;
Load3 = -0.15292
;unloading
Load4 = -0.09251
Load5 = -0.15513
Load6 = -0.22904
```

```
;unloading
Load7 = -0.16812
Load8 = -0.23295
Load9 = -0.33592
;unloading
Load10 = -0.25954
Load11 = -0.33600
Load12 = -0.4185
Load13 = -0.3353
Load14 = -0.2572
Load15 = -0.1837
Load16 = -0.1041
Load17 = -0.0099

end

```

Model File

```
;-----  
;-----Model-----  
;-----  
  
;-----Block-----  
  
poly brick @x1 @x2 @y1 @y2 @z1 @z2  
  
;-----Joints-----  
jset dd @dd1 dip @dip1 or @x1 @y1 @z1 n @num1 p @per1 s @sp1 id 1  
jset dd @dd2 dip @dip2 or @x1 @y1 @z1 n @num2 p @per2 s @sp2 id 2  
jset dd @dd3 dip @dip3 or @x1 @y1 @z1 n @num3 p @per3 s @sp3 id 3  
  
;----Grouping----  
group block 'cube' range z @z1 @z2  
  
;---Range Name---  
range name 'cube' z @z1 @z2  
  
;-----Mesh-----  
gen edge @edge
```

Material File

```

;-----
;--Material Properties--
;-----

change cons 2 range group 'cube'

prop mat 1 bc @bc bdi @bdi bfr @bfri bt @btension bu @bulk de @rho sh
@shear
prop jmat 1 jkn @jkn jks @jks jfri @phi jcoh @coh

change mat 1 range group 'cube'
change jmat 1 jcons @conj range group 'cube'

def matlist
  file = 'MatList.txt'
  status = open(file,1,1)

  Material = get_array(27) ; Array to read out material parameters

  Material(1)= conj      ; Joint Model
  Material(2)= jkn       ; joint normal stiffness [MPa]
  Material(3)= jks      ; joint shear stiffness [MPa]
  Material(4)= phi       ; joint friction angle [°]
  Material(5)= coh       ; joint cohesion [MPa]
  Material(6)= conm      ; Block Model
  Material(7)= rho       ; density
  Material(8)= pratio    ; Poisson's ratio [-]
  Material(9)= you       ; Youngs' modulus [MPa]
  Material(10)= bdi      ; dilatation angle [°]
  Material(11)= bfri     ; friction angle [°]
  Material(12)= btension ; tensile strength [MPa]
  Material(13)= bulk     ; bulk modulus [MPa]
  Material(14)= shear    ; shear modulus [MPa]
  Material(15)= bc       ; block cohesion [MPa]
  Material(16)= sp1*100  ; Spacing in x-direction [cm]
  Material(17)= sp2*100  ; Spacing in y-direction [cm]
  Material(18)= sp3*100  ; Spacing in z-direction[cm]
  Material(19)= dip1     ; Dip Angle [°]
  Material(20)= dip2     ; Dip Angle [°]

```

```
Material(21)= dip3      ; Dip Angle [°]
Material(22)= dd1      ; Dip Direction
Material(23)= dd2      ; Dip Direction
Material(24)= dd3      ; Dip Direction
Material(25)= per1     ; Persistence [-]
Material(26)= per2     ; Persistence [-]
Material(27)= per3     ; Persistence [-]

    status = write(Material,27)
status = close
end
@matlist
```

Load File

```
;-----  
;-----LOADING-----  
;-----  
  
def sys  
    md = 'C:\\...\\...\\' ; Folder location  
end  
@sys  
  
set directory @md  
  
define loading  
  
    array temp(1)  
    array Load(steps)  
  
;-----Loading-----  
;Redefinition of the applied displacements du to 3DEC adding them for  
each step  
  
    Load(1) = Load1  
    Load(2) = Load2-Load1  
    Load(3) = Load3-Load2  
    Load(4) = Load4-Load3  
    Load(5) = Load5-Load4  
    Load(6) = Load6-Load5  
    Load(7) = Load7-Load6  
    Load(8) = Load8-Load7  
    Load(9) = Load9-Load8  
    Load(10) =Load10-Load9  
    Load(11) =Load11-Load10  
    Load(12) =Load12-Load11  
    Load(13) =Load13-Load12  
    Load(14) =Load14-Load13  
    Load(15) =Load15-Load14  
    Load(16) =Load16-Load15  
    Load(17) =Load17-Load16  
  
loop p(1,steps)
```

```

v = Load(p)*pp
w = -1*v
fname="loadsteps-"+string(p)+"-"+string(name)+".3dsav"
command
    set directory @md
    bou zvel @v range z @z5 @z6
    bou zvel @w range z @z7 @z8

    step @cy
    ;solve ratio 1e-2
    ;solve r_type 1

endcommand

file = 'output.txt'
status = open(file,1,1)

boi = bou_head

loop while boi # 0
    boi_gp = bou_gp(boi)
;index of gridpoint associated with the boundary corner
    boi_zvel = bou_zvel(boi)
;y-applied velocity at boundary (just for control purpose)
    boi_zforce = bou_zforce(boi)
;y-applied or reaction force at boundary
    gpo_zdis = gp_zdis(boi_gp)
;y-displacement of gridpoint
    bv01 = gp_zreaction(boi_gp)
;returns y-reaction force for a gridpoint that has been assigned a zero-
;velocity boundary condition (just for control purpose)

    temp(1) = string(boi_gp) + ' ' +
string(boi_zvel) + ' ' + string(boi_zforce)
    temp(1) = temp(1) + ' ' + string(gpo_zdis)
    + ' ' + string(bv01)
    status = write(temp,1)

    boi = bou_next(boi)
endloop

```

```
        command
            save @fname
        endcommand
    end_loop
    status = close
end
@loading

def volume
    file = 'volume.txt' ;never ever use underscores in variable names
                        ;used for input-output functions!!!
    status = open(file,1,1)
    temp(1) = 'Number'+ ' '+'BlockIndex'+ ' '+'BlockID'+
'+BlockVolume'
    status = write(temp,1)

    bi = block_head
    ii = 1

    loop while bi # 0
        bvi = b_vol(bi)
        bid = b_id(bi)
        temp(1) = string(ii)+' '+'string(bi)+' '+'string(bid)+'
'+string(bvi)
        status = write(temp,1)
        bi = b_next(bi)
        ii = ii + 1
    endloop
    status = close
end
@volume

def loadlist
    file = 'LoadList.txt' ;File wenn sich die Lasten ändern
    status = open(file,1,1)
    status = write(Load,steps)
    status = close
end
@loadlist
```